J|A|C|S ARTICLES

Published on Web 07/06/2009

Mechanism of Helix Induction in Poly(4-carboxyphenyl isocyanide) with Chiral Amines and Memory of the Macromolecular Helicity and Its Helical Structures

Yoko Hase,[†] Kanji Nagai,[†,‡] Hiroki Iida,[†] Katsuhiro Maeda,[†] Noriaki Ochi,[†] Kyoichi Sawabe,[†] Koichi Sakajiri,[‡,||] Kento Okoshi,[*,‡,⊥] and Eiji Yashima[*,†,‡]

Department of Molecular Design and Engineering, Graduate School of Engineering, Nagoya University, Chikusa-ku, Nagoya 464-8603, Japan, and Yashima Super-structured Helix Project, Exploratory Research for Advanced Technology (ERATO), Japan Science and Technology Agency (JST), Japan

Received May 21, 2009; E-mail: kokoshi@polymer.titech.ac.jp; yashima@apchem.nagoya-u.ac.jp

Abstract: An optically inactive poly(4-carboxyphenyl isocyanide) (poly-**1**-**H**) changed its structure into the prevailing, one-handed helical structure upon complexation with optically active amines in dimethylsulfoxide (DMSO) and water, and the complexes show a characteristic induced circular dichroism in the polymer backbone region. Moreover, the macromolecular helicity induced in water and aqueous organic solutions containing more than 50 vol % water could be "memorized" even after complete removal of the chiral amines (***h***-poly-**1b**-**H**), while that induced in DMSO and DMSO−water mixtures containing less than 30 vol % water could not maintain the optical activity after removal of the chiral amines (poly-**1a**-**H**). We now report fully detailed studies of the helix induction mechanism with chiral amines and the memory of the macromolecular helicity in water and a DMSO−water mixture by various spectroscopic measurements, theoretical calculations, and persistence length measurements together with X-ray diffraction (XRD) measurements. From the spectroscopic results, such as circular dichroism (CD), absorption, IR, vibrational CD, and NMR of poly-**1a**-**H**, ***h***-poly-**1b**-**H**, and original poly-**1**-**H**, we concluded that the specific configurational isomerization around the C=N double bonds occurs during the helicity induction process in each solvent. In order to obtain the structural information, XRD measurements were done on the uniaxially oriented films of the corresponding methyl esters (poly-**1**-**Me**, poly-**1a**-**Me**, and ***h***-poly-**1b**-**Me**) prepared from their liquid crystalline polymer solutions. On the basis of the XRD analyses, the most plausible helical structure of poly-**1a**-**Me** was proposed to be a 9-unit/5-turn helix with two monomer units as a repeating unit, and that of ***h***-poly-**1b**-**Me** was proposed to be a 10-unit/3-turn helix consisting of one repeating monomer unit. The density functional theory calculations of poly(phenyl isocyanide), a model polymer of ***h***-poly-**1b**-**Me**, afforded a 7-unit/2-turn helix as the most possible helical structure, which is in good agreement with the XRD results. Furthermore, the persistence length measurements revealed that these structural changes accompany a significant change in the main-chain stiffness. The mechanism of helix induction in poly-**1**-**H** and the memory of the macromolecular helicity are discussed on the basis of these results.

Introduction

Optically active helical polymers with a controlled helix-sense have recently attracted considerable interest not only for mimicking biological helices but also for developing novel chiral materials.[1] In general, fully synthetic helical polymers can be prepared either by the polymerization of optically active monomers, such as isocyanates,[1a,c] silanes,[1d] and acetylenes,[1h,j−q] or by the helix-sense-selective polymerization of achiral or prochiral methacrylates,[1f] isocyanides,[2] and carbodiimides[3] bearing bulky substituents as the pendant groups using chiral catalysts or initiators. Although a number of helical polymers have been synthesized, the determination of their helical structures, including the helical pitch and handedness (right- or left-handed helix), remains very difficult but is quite important in order to develop more sophisticated chiral materials based on their macromolecular helicity.[1b,f,i]

Polyisocyanides are among the most extensively studied helical polymers since the pioneering research by Millich, Drenth, and Nolte.[2,4] The helical structure of polyisocyanides is considered to be a 4-unit/1-turn (4/1) helix when they have a bulky side group,[2c] which was first postulated by Millich on the basis of an X-ray analysis[2b] and later proposed experimentally by Nolte[5] and theoretically by Hoffmann.[6] The direct chromatographic resolution of poly(*tert*-butyl isocyanide) into enantiomeric helices clearly suggested a stable helical structure of polyisocyanides.[5,7] The resolved polymer with a positive rotation was postulated to have a left-handed helical conformation on the basis of a circular dichroism (CD) spectral analysis.[7] The stable helical con-

[†] Nagoya University.
[‡] ERATO, JST.
[||] Present address: Department of Chemistry, Faculty of Engineering, Gifu University, Yanagido, Gifu 501-1193, Japan.
[⊥] Present address: Department of Organic and Polymeric Materials, Graduate School of Science and Engineering, Tokyo Institute of Technology, 2-12-1, Ookayama, Meguro-ku, Tokyo 152-8552, Japan.

formation of the polyisocyanides in solution was further proved by the helix-sense-selective polymerization of achiral bulky isocyanides by Nolte[8] and Novak.[9] Since then, wide varieties of helical polyisocyanides with functional pendant groups have been synthesized, and some of them have been used for optoelectronic and liquid crystalline materials.[2,10]

However, Green[11] and Salvadori[12] claimed that polyisocyanides bearing less bulky aliphatic, aralkyl, and aromatic pendant groups might not have a regular 4/1 helical conformation because of a possible complicated configurational isomerism (*syn*−*anti* isomerization) around the C═N double bond and *s-cis* and *s-trans* conformational isomerism around the C−C bond of the main-chain. In addition, Euler and Rosen[13] experimentally showed a slow interconversion of poly(phenyl isocyanide) from an "as-prepared" 4/1 helical conformation to a more extended *s-trans*, zigzag conformation; an analogous *s-trans* structure as one of the most stable structures was also theoretically proposed by Clericuzio and Salvadori.[14] As a consequence, helical polyisocyanides—in particular, helical poly(phenyl isocyanide)s—lack unquestionable direct evidence for their helical structures.[15]

Recently, we reported that a helical polyisocyanide with a controlled helix-sense could be produced on the basis of the noncovalent "*helicity induction and chiral memory effect*".[1h,k,o,p,16] An optically inactive poly(4-carboxyphenyl isocyanide) (poly-**1**-**H**) and its sodium salt (poly-**1**-**Na**) were found to form a preferred-handed helical conformation upon noncovalent complexation with chiral amines in water.[17] The induced helix remained after complete removal of the chiral amines, and further modifications of the pendant groups to esters and amide residues were possible without loss of the macromolecular

(1) Reviews: (a) Green, M. M.; Peterson, N. C.; Sato, T.; Teramoto, A.; Cook, R.; Lifson, S. *Science* **1995**, *268*, 1860–1865. (b) Okamoto, Y.; Yashima, E. *Angew. Chem., Int. Ed.* **1998**, *37*, 1020–1043. (c) Green, M. M.; Park, J.-W.; Sato, T.; Teramoto, A.; Lifson, S.; Selinger, R. L. B.; Selinger, J. V. *Angew. Chem., Int. Ed.* **1999**, *38*, 3138–3154. (d) Fujiki, M. *Macromol. Rapid Commun.* **2001**, *22*, 539–563. (e) Hill, D. J.; Mio, M. J.; Prince, R. B.; Hughes, T. S.; Moore, J. S. *Chem. Rev.* **2001**, *101*, 3893–4011. (f) Nakano, T.; Okamoto, Y. *Chem. Rev.* **2001**, *101*, 4013–4038. (g) Brunsveld, L.; Folmer, B. J. B.; Meijer, E. W.; Sijbesma, R. P. *Chem. Rev.* **2001**, *101*, 4071–4097. (h) Yashima, E.; Maeda, K.; Nishimura, T. *Chem.−Eur. J.* **2004**, *10*, 42–51. (i) Reggelin, M.; Doerr, S.; Klussmann, M.; Schultz, M.; Holbach, M. *Proc. Natl. Acad. Sci. U.S.A.* **2004**, *101*, 5461–5466. (j) Lam, J. W. Y.; Tang, B. Z. *Acc. Chem. Res.* **2005**, *38*, 745–754. (k) Maeda, K.; Yashima, E. *Top. Curr. Chem.* **2006**, *265*, 47–88. (l) Aoki, T.; Kaneko, T.; Teraguchi, M. *Polymer* **2006**, *47*, 4867–4892. (m) Masuda, T. *J. Polym. Sci., Part A: Polym. Chem.* **2007**, *45*, 165–180. (n) Rudick, J. G.; Percec, V. *New J. Chem.* **2007**, *31*, 1083–1096. (o) Yashima, E.; Maeda, K. *Macromolecules* **2008**, *41*, 3–12. (p) Yashima, E.; Maeda, K.; Furusho, Y. *Acc. Chem. Res.* **2008**, *41*, 1166–1180. (q) Rudick, J. G.; Percec, V. *Acc. Chem. Res.* **2008**, *41*, 1641–1652. (r) Pijper, D.; Feringa, B. L. *Soft Matter* **2008**, *4*, 1349–1372. (s) Kim, H.-J.; Lim, Y.-B.; Lee, M. *J. Polym Sci., Part A: Polym. Chem.* **2008**, *46*, 1925–1935.

(2) Reviews: (a) Millich, F. *Chem. Rev.* **1972**, *72*, 101–113. (b) Millich, F. *Adv. Polym. Sci.* **1975**, *19*, 117–141. (c) Drenth, W.; Nolte, R. J. M. *Acc. Chem. Res.* **1979**, *12*, 30–35. (d) Millich, F. *J. Polym. Sci. Macromol. Rev.* **1980**, *15*, 207–253. (e) Nolte, R. J. M. *Chem. Soc. Rev.* **1994**, *23*, 11–19. (f) Takahashi, S.; Onitsuka, K.; Takei, F. *Proc. Jpn. Acad. Ser. B* **1998**, *74*, 25–30. (g) Cornelissen, J. J. L. M.; Rowan, A. E.; Nolte, R. J. M.; Sommerdijk, N. A. J. M. *Chem. Rev.* **2001**, *101*, 4039–4070. (h) Suginome, M.; Ito, Y. *Adv. Polym. Sci.* **2004**, *171*, 77–136. (i) Amabilino, D. B.; Serrano, J.-L.; Sierra, T.; Veciana, J. *J. Polym. Sci., Part A: Polym. Chem.* **2006**, *44*, 3161–3174.

(3) (a) Tian, G.; Lu, Y.; Novak, B. M. *J. Am. Chem. Soc.* **2004**, *126*, 4082–4083. (b) Tang, H.-Z.; Novak, B. M.; He, J.; Polavarapu, P. L. *Angew. Chem., Int. Ed.* **2005**, *44*, 7298–7301. (c) Tang, H.-Z.; Boyle, P. D.; Novak, B. M. *J. Am. Chem. Soc.* **2005**, *127*, 2136–2142.

(4) (a) Millich, F.; Sinclair, R. G. *J. Polym. Sci., Part C* **1968**, *22*, 33–43. (b) Nolte, R. J. M.; Zwikker, J. W.; Reedijk, J.; Drenth, W. *J. Mol. Catal.* **1978**, *4*, 423–426. (c) van Beijnen, A. J. M.; Nolte, R. J. M.; Zwikker, J. W.; Drenth, W. *J. Mol. Catal.* **1978**, *4*, 427–432.

(5) Nolte, R. J. M.; van Beijnen, A. J. M.; Drenth, W. *J. Am. Chem. Soc.* **1974**, *96*, 5932–5933.

(6) Kollmar, C.; Hoffmann, R. *J. Am. Chem. Soc.* **1990**, *112*, 8230–8238.

(7) van Beijnen, A. J. M.; Nolte, R. J. M.; Drenth, W.; Hezemans, A. M. F. *Tetrahedron* **1976**, *32*, 2017–2019.

(8) (a) Kamer, P. C. J.; Nolte, R. J. M.; Drenth, W. *J. Chem. Soc., Chem. Commun.* **1986**, 1789–1791. (b) Kamer, P. C. J.; Nolte, R. J. M.; Drenth, W. *J. Am. Chem. Soc.* **1988**, *110*, 6818–6825.

(9) Deming, T. J.; Novak, B. M. *J. Am. Chem. Soc.* **1992**, *114*, 7926–7927.

(10) For liquid crystalline polyisocyanides: (a) Cornelissen, J. J. L. M.; Donners, J. J. J. M.; de Gelder, R.; Graswinckel, W. S.; Metselaar, G. A.; Rowan, A. E.; Sommerdijk, N. A. J. M.; Nolte, R. J. M. *Science* **2001**, *293*, 676–680. (b) Cornelissen, J. J. L. M.; Granswinckel, W. S.; Rowan, A. E.; Sommerdijk, N. A. J. M.; Nolte, R. J. M. *J. Polym. Sci., Part A: Polym. Chem.* **2003**, *41*, 1725–1736. (c) Tian, Y.; Kamata, K.; Yoshida, H.; Iyoda, T. *Chem.-Eur. J.* **2006**, *12*, 584–591. (d) Kajitani, T.; Okoshi, K.; Sakurai, S.-i.; Kumaki, J.; Yashima, E. *J. Am. Chem. Soc.* **2006**, *128*, 708–709. (e) Wezenberg, S. J.; Metselaar, G. A.; Rowan, A. E.; Cornelissen, J. J. L. M.; Seebach, D.; Nolte, R. J. M. *Chem.-Eur. J.* **2006**, *12*, 2778–2786. (f) Metselaar, G. A.; Adams, P. J. H. M.; Nolte, R. J. M.; Cornelissen, J. J. L. M.; Rowan, A. E. *Chem.-Eur. J.* **2007**, *13*, 950–960. (g) Metselaar, G. A.; Wezenberg, S. J.; Cornelissen, J. J. L. M.; Nolte, R. J. M.; Rowan, A. E. *J. Polym. Sci., Part A: Polym. Chem.* **2007**, *45*, 981–988. (h) Onouchi, H.; Okoshi, K.; Kajitani, T.; Sakurai, S.-i.; Nagai, K.; Kumaki, J.; Onitsuka, K.; Yashima, E. *J. Am. Chem. Soc.* **2008**, *130*, 229–236. (i) Kajitani, T.; Lin, H.; Nagai, K.; Okoshi, K.; Onouchi, H.; Yashima, E. *Macromolecules* **2009**, *42*, 560–567. For optoelectronic polyisocyanides, see: (j) Kauranen, K.; Verbiest, T.; Boutton, C.; Teerenstra, M. N.; Schouten, A. J.; Nolte, R. J. M.; Persoons, A. *Science* **1995**, *270*, 966–969. (k) Hida, N.; Takei, F.; Onitsuka, K.; Shiga, K.; Asaoka, S.; Iyoda, T.; Takahashi, S. *Angew. Chem., Int. Ed.* **2003**, *42*, 4349–4352. For other leading references on helical polyisocyanides prepared by the polymerization of the corresponding optically active monomers, see: (l) Cornelissen, J. J. L. M.; Fischer, M.; Sommerdijk, N. A. J. M.; Nolte, R. J. M. *Science* **1998**, *280*, 1427–1430. (m) Amabilino, D. B.; Ramos, E.; Serrano, J.-L.; Sierra, T.; Veciana, J. *J. Am. Chem. Soc.* **1998**, *120*, 9126–9134. (n) Amabilino, D. B.; Ramos, E.; Serrano, J.-L.; Veciana, J. *Adv. Mater.* **1998**, *10*, 1001–1005. (o) Hasegawa, T.; Kondoh, S.; Matsuura, K.; Kobayashi, K. *Macromolecules* **1999**, *32*, 6595–6603. (p) Takei, F.; Yanai, K.; Onitsuka, K.; Takahashi, S. *Chem.−Eur. J.* **2000**, *6*, 983–993. (q) Cornelissen, J. J. L. M.; Graswinckel, W. S.; Adams, P. J. H. M.; Nachtegaal, G. H.; Kentgens, A. P. M.; Sommerdijk, N. A. J. M.; Nolte, R. J. M. *J. Polym. Sci., Part A: Polym. Chem.* **2001**, *39*, 4255–4264. (r) Yamada, Y.; Kawai, T.; Abe, J.; Iyoda, T. *J. Polym. Sci., Part A: Polym. Chem.* **2002**, *40*, 399–408. (s) Takei, F.; Onitsuka, K.; Takahashi, S. *Macromolecules* **2005**, *38*, 1513–1516. (t) Kajitani, T.; Okoshi, K.; Yashima, E. *Macromolecules* **2008**, *41*, 1601–1611.

(11) Green, M. M.; Gross, R. A.; Schilling, F. C.; Zero, K.; Crosby, C. *Macromolecules* **1988**, *21*, 1839–1846.

(12) Pini, D.; Iuliano, A.; Salvadori, P. *Macromolecules* **1992**, *25*, 6059–6062.

(13) (a) Spencer, L.; Kim, M.; Euler, W. B.; Rosen, W. *J. Am. Chem. Soc.* **1997**, *119*, 8129–8130. (b) Euler, W. B.; Huang, J.-T.; Kim, M.; Spencer, L.; Rosen, W. *Chem. Commun.* **1997**, 257–258. (c) Huang, J.-T.; Sun, J.; Euler, W. B.; Rosen, W. *J. Polym. Sci., Part A, Polym. Chem.* **1997**, *35*, 439–446. (d) Spencer, L.; Euler, W. B.; Traficante, D. D.; Kim, M.; Rosen, W. *Magn. Reson. Chem.* **1998**, *36*, 398–402.

(14) (a) Clericuzio, M.; Alagona, G.; Ghio, C.; Salvadori, P. *J. Am. Chem. Soc.* **1997**, *119*, 1059–1071. Molecular orbital calculations of poly(iminomethylene) using semi-empirical methods were also conducted. See: (b) Young, V. Y.; Hellmuth, E. W. *J. Mol. Struct.: THEOCHEM* **2002**, *578*, 1–17.

(15) Recently, we have reported the helix-sense-selective living polymerization of an optically active phenyl isocyanide bearing an L-alanine pendant with a long decyl chain with the achiral μ-ethynediyl Pt−Pd catalyst that unprecedentedly produced both right- and left-handed helical, rigid-rod polyisocyanides at once with a different molecular weight and a narrow molecular weight distribution, which could be separated into each helix in a facile fractionation with acetone. The structures of both right- and left-handed helical polyisocyanides were proposed to be a 15-unit/4-turn (15/4) helix on the basis of X-ray analyses of the corresponding oriented films.[10h] However, the detailed structural analysis, including a possible configurational and conformational isomerism of the main-chain, has never been pursued.

helicity memory.[18] However, the helical structures of poly-**1**-**H** induced by chiral amines in water and aqueous organic solutions containing more than 50 vol % water can be effectively memorized after complete removal of the chiral amines (***h***-poly-**1b**-**H**), while the helical structures of poly-**1**-**H** induced by chiral amines in dimethylsulfoxide (DMSO)[19] and DMSO−water mixtures containing less than 30 vol % water cannot maintain their helicity after removal of the chiral amines (poly-**1a**-**H**; Figure 1).[20] These results raise questions as to what different helical structures the polyisocyanide can form in DMSO and water in the presence of chiral amines and why the helical structure induced in DMSO cannot be memorized after removal of the chiral amines.

To address these questions, we synthesized a series of isotopically labeled poly-**1**-**H**'s and their methyl esters (poly-**1**-**Me**'s) with deuterium (D), ^{13}C, and ^{15}N (Chart 1) and nonlabeled poly-**1**-**H** and poly-**1**-**Me**, and their structures before and after the helicity induction with chiral amines in water and organic solvent−water mixtures and subsequent memory were investigated in detail by absorption, CD, IR, vibrational CD (VCD), and NMR spectroscopies together with X-ray diffraction (XRD) of the oriented films prepared from nematic and cholesteric liquid crystalline (LC) poly-**1**-**Me**'s, persistence length measurements, and theoretical calculations. These results shed light on the mechanism of helicity induction in poly-**1** and subsequent memory of the macromolecular helicity.

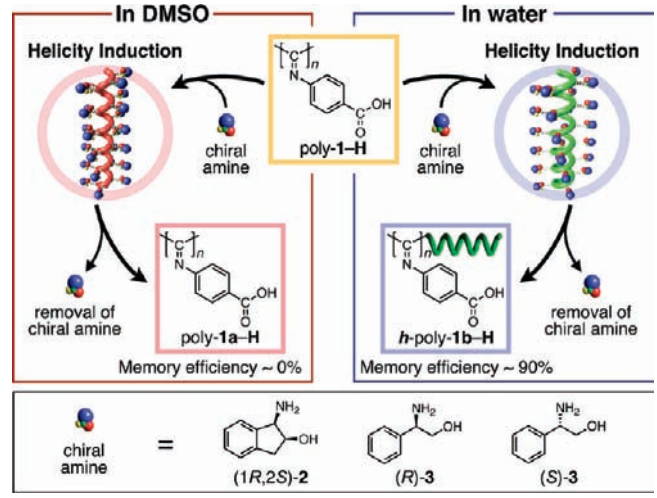

Figure 1. Schematic illustration of helicity induction in poly-**1**-**H** in DMSO and water with chiral amines (**2** or **3**) and after subsequent removal of the chiral amines. The macromolecular helicity induced in water is memorized after complete removal of the chiral amines (***h***-poly-**1b**-**H**), whereas that induced in DMSO cannot be memorized (poly-**1a**-**H**).

Results and Discussion

Synthesis and Polymerization of Isotopically Labeled Monomers. Four novel isotopically labeled sodium 4-isocyanobenzoates (**1**-**Na**-d_4, **1**-**Na**-^{13}C, **1**-**Na**-d_4-^{13}C, and **1**-**Na**-^{15}N) were prepared as outlined in Schemes S1−S4 (Supporting Information). The structures of the obtained isocyanides were characterized by IR, NMR, and mass spectroscopy, and they were in fair agreement with their assigned structures (see the Supporting Information). The polymerization of **1**-**Na**, **1**-**Na**-d_4, **1**-**Na**-^{13}C, **1**-**Na**-d_4-^{13}C, and **1**-**Na**-^{15}N was performed in water with $NiCl_2 \cdot 6H_2O$ as the catalyst as previously reported, affording the corresponding polyisocyanides in good yields, poly-**1**-**H**, poly-**1**-**H**-d_4, poly-**1**-**H**-^{13}C, poly-**1**-**H**-d_4-^{13}C, and poly-**1**-**H**-^{15}N, respectively (Scheme 1A, Chart 1, and Table 1).[17] The number-average molecular weights (M_n) of their methyl esters, as determined by size exclusion chromatography (SEC) with polystyrene standards using chloroform ($CHCl_3$) as the eluent, were relatively low (2.6×10^4−3.5×10^4) (runs 1−5 in Table 1). However, when the polymerization of 4-(ethoxycarbonyl)phenyl isocyanide (**1**-**Et**) was performed in dry tetrahydrofuran (THF) containing a small amount of alcohols, such as methanol (MeOH) (THF−MeOH = 99:1, v/v), with the same $NiCl_2 \cdot 6H_2O$ catalyst, we found that a higher molecular weight poly-**1**-**Et** (HMW-poly-**1**-**Et**; $M_n = 8.6 \times 10^4$) was obtained in 88% yield (run 6 in Table 1 and Scheme 1B).[21] The obtained HMW-poly-**1**-**Et** was further alkaline hydrolyzed, followed by esterification with CH_2N_2 to give HMW-poly-**1**-**H** and HMW-poly-**1**-**Me**, respectively (Scheme 1B).

Macromolecular Helicity Induction in Poly-1-H with Chiral Amines and Isolation of the Polymers. Poly-**1**-**H** and the isotopically labeled poly-**1**-**H**'s (poly-**1**-**H**-d_4, poly-**1**-**H**-^{13}C, poly-**1**-**H**-d_4-^{13}C, and poly-**1**-**H**-^{15}N) were then annealed with (1*R*,2*S*)-**2** in DMSO−water (9:1 or 4:1, v/v) and (*R*)- or (*S*)-**3** in water, acetonitrile (CH_3CN)−water (1:1, v/v), or 2-propanol−water (1:1, v/v) at 50 °C for 3−72 days, as reported previously.[17,20] Figure 2 shows the typical CD and absorption spectra of the poly-**1**-**H**−(1*R*,2*S*)-**2** complex in DMSO−water

(16) (a) Yashima, E.; Maeda, K.; Okamoto, Y. *Nature* **1999**, *399*, 449–451. (b) Maeda, K.; Morino, K.; Okamoto, Y.; Sato, T.; Yashima, E. *J. Am. Chem. Soc.* **2004**, *126*, 4329–4342. (c) Morino, K.; Watase, N.; Maeda, K.; Yashima, E. *Chem.−Eur. J.* **2004**, *10*, 4703–4707. (d) Onouchi, H.; Kashiwagi, D.; Hayashi, K.; Maeda, K.; Yashima, E. *Macromolecules* **2004**, *37*, 5495–5503. (e) Onouchi, H.; Miyagawa, T.; Furuko, A.; Maeda, K.; Yashima, E. *J. Am. Chem. Soc.* **2005**, *127*, 2960–2965. (f) Miyagawa, T.; Furuko, A.; Maeda, K.; Katagiri, H.; Furusho, Y.; Yashima, E. *J. Am. Chem. Soc.* **2005**, *127*, 5018–5019. (g) Onouchi, H.; Hasegawa, T.; Kashiwagi, D.; Ishiguro, H.; Maeda, K.; Yashima, E. *Macromolecules* **2005**, *38*, 8625–8633. (h) Hasegawa, T.; Morino, K.; Tanaka, Y.; Katagiri, H.; Furusho, Y.; Yashima, E. *Macromolecules* **2006**, *39*, 482–488. (i) Hasegawa, T.; Maeda, K.; Ishiguro, H.; Yashima, E. *Polym. J.* **2006**, *38*, 912–919. (j) Kawauchi, T.; Kumaki, J.; Kitaura, A.; Okoshi, K.; Kusanagi, H.; Kobayashi, K.; Sugai, T.; Shinohara, H.; Yashima, E. *Angew. Chem., Int. Ed.* **2008**, *47*, 515–519. (k) Kawauchi, T.; Kitaura, A.; Kumaki, J.; Kusanagi, H.; Yashima, E. *J. Am. Chem. Soc.* **2008**, *130*, 11889–11891. For chiral memory effect of other macromolecular and supramolecular systems, see: (l) Furusho, Y.; Kimura, T.; Mizuno, Y.; Aida, T. *J. Am. Chem. Soc.* **1997**, *119*, 5267–5268. (m) Mizuno, T.; Takeuchi, M.; Hamachi, I.; Nakashima, K.; Shinkai, S. *J. Chem. Soc., Perkin Trans. 2* **1998**, 2281–2288. (n) Bellacchio, E.; Lauceri, R.; Gurrieri, S.; Scolaro, L. M.; Romeo, A.; Purrello, R. *J. Am. Chem. Soc.* **1998**, *120*, 12353–12354. (o) Prins, L. J.; Jong, F. D.; Timmerman, P.; Reinhoudt, D. N. *Nature* **2000**, *408*, 181–184. (p) Kubo, Y.; Ohno, T.; Yamanaka, J.-i.; Tokita, S.; Iida, T.; Ishimaru, Y. *J. Am. Chem. Soc.* **2001**, *123*, 12700–12701. (q) Lauceri, R.; Raudino, A.; Scolaro, L. M.; Micali, N.; Purrello, R. *J. Am. Chem. Soc.* **2002**, *124*, 894–895. (r) Mammana, A.; D'Urso, A.; Lauceri, R.; Purrello, R. *J. Am. Chem. Soc.* **2007**, *129*, 8062–8063. (s) Rosaria, L.; D'Urso, A.; Mammana, A.; Purrello, R. *Chirality* **2008**, *20*, 411–419. (t) Ousaka, N.; Inai, Y.; Kuroda, R. *J. Am. Chem. Soc.* **2008**, *130*, 12266–12267.

(17) Ishikawa, M.; Maeda, K.; Mitsutsuji, Y.; Yashima, E. *J. Am. Chem. Soc.* **2004**, *126*, 732–733.

(18) (a) Hase, Y.; Mitsutsuji, Y.; Ishikawa, M.; Maeda, K.; Okoshi, K.; Yashima, E. *Chem. Asian J.* **2007**, *2*, 755–763. (b) Miyabe, T.; Hase, Y.; Iida, H.; Maeda, K.; Yashima, E. *Chirality* **2009**, *21*, 44–50.

(19) Ishikawa, M.; Maeda, K.; Yashima, E. *J. Am. Chem. Soc.* **2002**, *124*, 7448–7458.

(20) Hase, Y.; Ishikawa, M.; Muraki, R.; Maeda, K.; Yashima, E. *Macromolecules* **2006**, *39*, 6003–6008.

(21) The effect of MeOH on the polymerization of **1**-**Et** with $NiCl_2 \cdot 6H_2O$ remains obscure, but this method may be useful to obtain high-molecular-weight polyisocyanides.

Chart 1. Structures of Poly(phenyl isocyanide) Derivatives

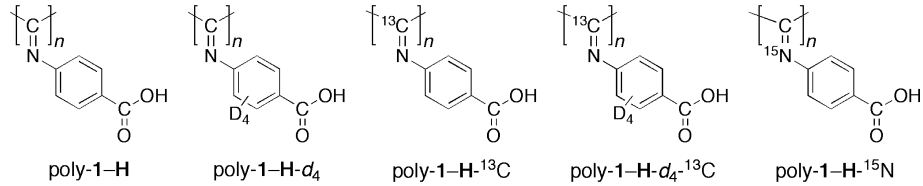

Scheme 1. Synthesis of Poly(phenyl isocyanide) Derivatives

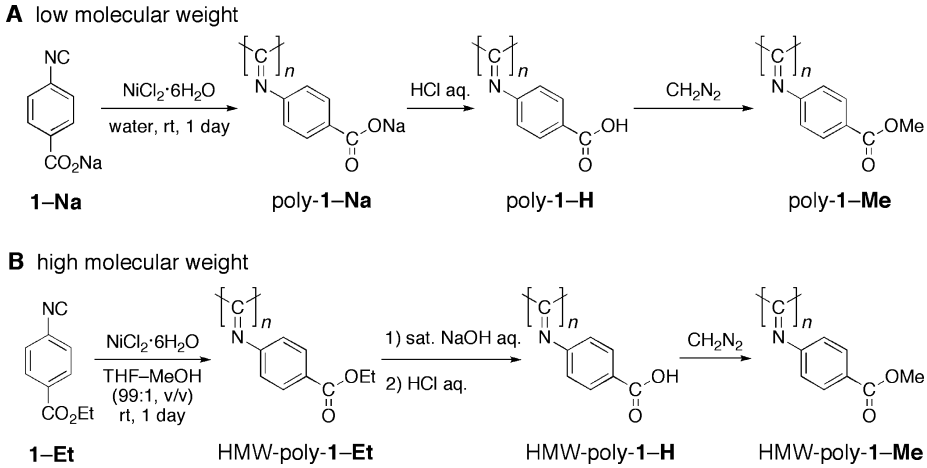

Table 1. Polymerization Results of **1-Na**, **1-Na**-d_4, **1-Na**-^{13}C, **1-Na**-d_4-^{13}C, **1-Na**-^{15}N, and **1-Et** with $NiCl_2 \cdot 6H_2O$[a]

run	monomer	yield (%)[b]	$M_n \times 10^{-4}$ (M_w/M_n)[c]	polymer
1	**1-Na**	90	3.5 (3.2)	poly-**1-H**
2	**1-Na**-d_4	66	2.6 (2.4)	poly-**1-H**-d_4
3	**1-Na**-^{13}C	82	2.7 (2.8)	poly-**1-H**-^{13}C
4	**1-Na**-d_4-^{13}C	78	2.8 (2.5)	poly-**1-H**-d_4-^{13}C
5	**1-Na**-^{15}N	62	2.7 (5.8)	poly-**1-H**-^{15}N
6	**1-Et**[d]	88	8.6 (5.0)[e]	HMW-poly-**1-H**

[a] Polymerized in water under air at room temperature for 1 day. [**1-Na**] = 0.5 M; [**1-Na**]/[$NiCl_2 \cdot 6H_2O$] = 100. [b] MeOH-insoluble part. [c] Determined by SEC (polystyrene standards) with $CHCl_3$ as the eluent as its methyl ester. [d] Polymerized in THF−MeOH (99:1, v/v) under nitrogen at room temperature for 1 day. [**1-Et**] = 0.1 M; [**1-Et**]/[$NiCl_2 \cdot 6H_2O$] = 100. [e] Determined by SEC (polystyrene standards) with $CHCl_3$ as the eluent as its ethyl ester.

(9:1, v/v) (a and c in Figure 2A) and the poly-**1-H**−(*R*)-**3** complex in CH_3CN−water (1:1, v/v) (e and g in Figure 2B). Both polymers formed a predominantly one-handed helix and exhibited an induced CD (ICD) in the imino chromophore region of the polymer backbones (300−450 nm), and their CD spectral patterns and λ_{max} of the Cotton effects were similar to each other, although their absorption spectra (c and g in Figure 2) were slightly different from one another. As previously reported,[17,20] the helicity of poly-**1-H**'s (***h***-poly-**1b-H**'s) induced by (*R*)-**3** in water and aqueous organic solutions containing more than 50 vol % water was automatically memorized during the helicity induction process, thus showing an intense ICD after complete removal of the chiral amine (see f in Figure 2B and run 4 in Table 2), whereas the optical activity induced in the poly-**1-H**'s by (1*R*,2*S*)-**2** in DMSO−water (9:1, v/v) almost completely disappeared after removal of the chiral amine (poly-**1a-H**'s) (see b in Figure 2A and run 1 in Table 2).[20] We observed a significant difference in the absorption spectra between ***h***-poly-**1b-H** and poly-**1a-H** (d and h in Figure 2 and Figure 2C); the absorption intensity of ***h***-poly-**1b-H** in the pendant aromatic region (λ_{max} = 251 nm) was reduced by 18% (hypochromic effect), while that in the main-chain imino chromophore region (λ = ca. 360 nm) was increased by ca. 20% (hyperchromic effect), as compared with the values for poly-**1a-H**. These results suggested intramolecular stacking of the aromatic pendant groups of ***h***-poly-**1b-H** and also a difference in their main-chain structure, which will be discussed later in detail.

The chiroptical properties of the poly-**1-H**'s after helicity induction in different solvents followed by removal of the chiral amines are summarized in Table 2. All the helical ***h***-poly-**1b-H**'s induced in water and CH_3CN− or 2-propanol−water (1:1, v/v) maintained their induced helical structures after complete removal of the chiral amines, and the memory efficiencies thus estimated on the basis of the $\Delta\varepsilon$ values of the polymers before isolation were greater than 85%; their absolute $\Delta\varepsilon$ values at ca. 360 nm after isolation were in the range of 9.28−11.9 in alkaline water (Table 2), indicating that the isotope effects on helicity induction and subsequent memory of the helicity could be negligible. The CD intensity tended to increase with an increase in the molecular weight of ***h***-poly-**1b-H** and HMW-***h***-poly-**1b-H** (runs 2−4, 15, and 16 in Table 2). A similar molecular weight effect on the helicity induction was also observed for the dynamic helical poly((4-carboxyphenyl)acetylene) upon complexation with chiral amines in DMSO.[16b] As previously reported,[17] ***h***-poly-**1b-H**'s can be converted to the corresponding methyl esters (***h***-poly-**1b-Me**'s) without loss of macromolecular helicity. On the other hand, poly-**1-H**, poly-**1-H**-^{13}C, poly-**1-H**-^{15}N, and HMW-poly-**1-H** induced in DMSO−water (9:1 or 4:1, v/v) with (1*R*,2*S*)-**2** could not retain their optical activity after removal of the chiral amine (runs 1, 7, 12, and 14 in Table 2).

NMR Studies. The ^{1}H, ^{13}C, and ^{15}N NMR spectra of the original poly-**1-H**, poly-**1-H**-^{13}C, and poly-**1-Me**-^{15}N derived from poly-**1-H**-^{15}N and those of the corresponding helical polymers during the helicity induction with chiral amines in different solvents and after removal of the chiral amines were then measured to gain insight into the changes in the structures

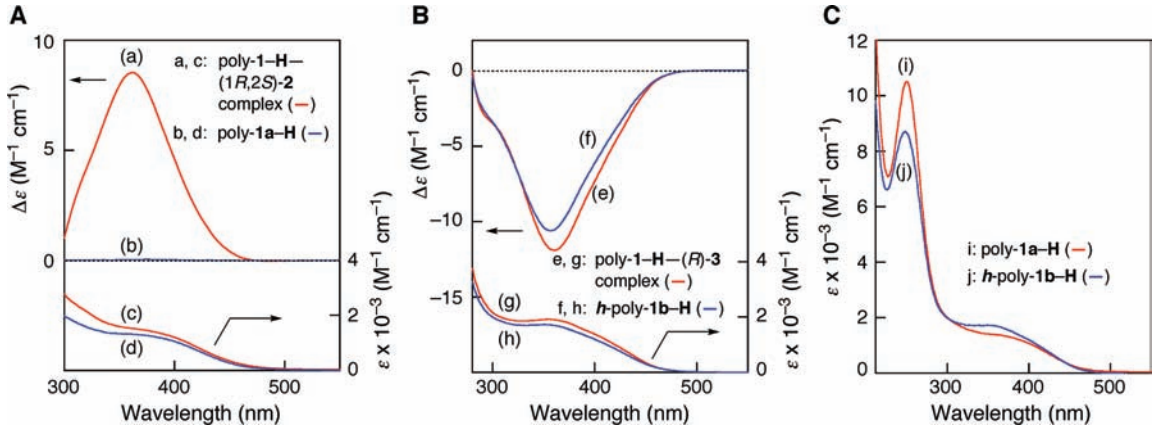

Figure 2. (A,B) CD and absorption spectra of poly-**1**-**H**−(1*R*,2*S*)-**2** complex in DMSO−water (9:1, v/v) (run 1 in Table 2) (a,c), poly-**1**-**H**−(*R*)-**3** complex in CH_3CN−water (1:1, v/v) (run 4 in Table 2) (e,g), and poly-**1a**-**H** (run 1 in Table 2) (b,d) and ***h***-poly-**1b**-**H** (run 4 in Table 2) (f,h) after complete removal of (1*R*,2*S*)-**2** and (*R*)-**3**, respectively, measured in alkaline water ([polymer]/[NaOH] = 1) at ambient temperature; [polymer] = 1.0 mg/mL. (C) Absorption spectra of poly-**1a**-**H** (run 1 in Table 2) (i) and ***h***-poly-**1b**-**H** (run 4 in Table 2) (j), measured in alkaline water ([polymer]/[NaOH] = 1) at ambient temperature; [polymer] = 1.0 mg/mL.

Table 2. CD Spectral Data of Helical Poly-**1**-**H**'s Induced by (1*R*,2*S*)-**2** in DMSO−Water (9:1 or 4:1, v/v) and by **3** in Water and Organic Solvent−Water (1:1, v/v) and Isolated Polymers and Their Methyl Esters after Removal of Chiral Amines[a]

					after removal of chiral amines			poly-**1**-**Me**
run	polymer	chiral amine	solvent (v/v)	Δε (λ, time)[b]		Δε (λ)[c]	memory efficiency (%)[d]	Δε (λ)[e]
1	poly-**1**-**H**	(1*R*,2*S*)-**2**	DMSO−water (9/1)	+8.53 (362, 3)	poly-**1a**-**H**	+0.04 (360)	0.5	ca. 0
2	poly-**1**-**H**	(*R*)-**3**	water	−11.1 (360, 46)	***h***-poly-**1b**-**H**	−10.3 (357)	92	
3	poly-**1**-**H**	(*S*)-**3**	water	+12.0 (360, 55)	***h***-poly-**1b**-**H**	+10.6 (357)	88	+11.6 (360)
4	poly-**1**-**H**	(*R*)-**3**	CH_3CN−water (1/1)	−11.9 (360, 15)[f]	***h***-poly-**1b**-**H**	−10.6 (357)	89	−11.8 (360)
5	poly-**1**-**H**-d_4	(*R*)-**3**	CH_3CN−water (1/1)	−10.7 (360, 17)[f]	***h***-poly-**1b**-**H**-d_4	−9.65 (356)	90	−9.16 (360)
6	poly-**1**-**H**-d_4	(*S*)-**3**	CH_3CN−water (1/1)	+11.7 (360, 17)[f]	***h***-poly-**1b**-**H**-d_4	+10.4 (357)	89	+9.59 (359)
7	poly-**1**-**H**-^{13}C	(1*R*,2*S*)-**2**	DMSO-d_6−D_2O (9/1)	+9.48 (362, 33)[g]	poly-**1a**-**H**-^{13}C	+0.05 (360)	0.5	ca. 0
8	poly-**1**-**H**-^{13}C	(*R*)-**3**	D_2O	−12.7 (360, 33)	***h***-poly-**1b**-**H**-^{13}C	−11.9 (357)	94	
9	poly-**1**-**H**-^{13}C	(*R*)-**3**	CH_3CN−water (1/1)	−12.3 (360, 16)[f]	***h***-poly-**1b**-**H**-^{13}C	−10.8 (358)	88	−12.8 (360)
10	poly-**1**-**H**-d_4-^{13}C	(*R*)-**3**	CH_3CN−water (1/1)	−9.97 (360, 17)[f]	***h***-poly-**1b**-**H**-d_4-^{13}C	−9.28 (357)	93	−8.88 (359)
11	poly-**1**-**H**-d_4-^{13}C	(*S*)-**3**	CH_3CN−water (1/1)	+10.4 (360, 17)[f]	***h***-poly-**1b**-**H**-d_4-^{13}C	+9.63 (357)	93	+8.08 (360)
12	poly-**1**-**H**-^{15}N	(1*R*,2*S*)-**2**	DMSO−water (9/1)	+8.79, (362, 3)	poly-**1a**-**H**-^{15}N	+0.04 (360)	0.5	ca. 0
13	poly-**1**-**H**-^{15}N	(*R*)-**3**	CH_3CN−water (1/1)	−11.8 (359, 17)[f]	***h***-poly-**1b**-**H**-^{15} N	−10.9 (357)	92	−11.0 (360)
14	HMW-poly-**1**-**H**	(1*R*,2*S*)-**2**	DMSO−water (4/1)	+7.21 (362, 5)	HMW-poly-**1a**-**H**	+0.12 (362)	1.6	+0.04 (360)
15	HMW-poly-**1**-**H**	(*R*)-**3**	CH_3CN−water (1/1)	−14.7 (360, 21)[f]	HMW-***h***-poly-**1b**-**H**	−12.9 (357)	88	−12.0 (360)
16	HMW-poly-**1**-**H**	(*R*)-**3**	2-propanol−water (1/1)	−17.9 (357, 72)[f]	HMW-***h***-poly-**1b**-**H**	−15.2 (360)	85	−14.9 (359)

[a] The concentration of polymers is 1.0 mg/mL. [b] Measured at ambient temperature (20−25 °C) after the samples had been allowed to stand at 50 °C for days; molar ratio of an amine to monomeric units of poly-**1**-**H**'s is 10; Δε (M^{-1} cm^{-1}), λ (nm), and time (days). [c] Measured in alkaline water ([NaOH]/[polymer] = 1 and [polymer] = 1.0 mg/mL); Δε (M^{-1} cm^{-1}) and λ (nm). [d] Estimated on the basis of the ICD values of poly-**1**-amine complexes before isolation. [e] Measured in $CHCl_3$ ([polymer] = 1.0 mg/mL); Δε (M^{-1} cm^{-1}) and λ (nm). [f] Molar ratio of an amine to monomeric units of poly-**1**-**H** is 20. [g] After 14 days, the poly-**1**-**H**-^{13}C−(1*R*,2*S*)-**2** complex showed $\Delta\varepsilon_{362} = +9.33$.

of the poly-**1**-**H**'s (Figure 3). The ^{1}H, ^{13}C, and ^{15}N NMR spectra showed considerable differences in their patterns. In particular, the changes in the structures of poly-**1**-**H**-^{13}C before and after the helix formation upon complexation with (1*R*,2*S*)-**2** in DMSO-d_6−D_2O (9:1, v/v) (e) and (*R*)-**3** in D_2O (g) were most clearly observed in their ^{13}C NMR spectra (Figure 3B). The original poly-**1**-**H**-^{13}C exhibited rather broad and complicated signals composed of at least three signals with different intensities centered at 160.7, 161.9, and 162.8 ppm due to the main-chain C═N carbon resonances, which can be ascribed to some stereoirregularity of the main-chain for triad tacticity due to the *syn*−*anti* isomerism and/or conformationally different segments (*s-cis* and *s-trans*) (Chart 2). However, interestingly, the ^{13}C NMR spectra of the poly-**1**-**H**-^{13}C complexed with (1*R*,2*S*)-**2** in DMSO-d_6−D_2O (9:1, v/v) and (*R*)-**3** in D_2O after helicity induction (the molar ellipticity at the first Cotton effect ($\Delta\varepsilon_{first}$) was +9.33 and −12.7, respectively) exhibited sharp signals centered at 162.8 and 160.9 ppm, respectively, suggesting selective configurational isomerization around the C═N double bonds (*syn*−*anti* isomerization) (Chart 2C) which may take place during the helix formation.[17,19] More interestingly, these sharp signals remained even after removal of the chiral amines (f and h), although the former polymer immediately lost its optical activity, while the latter maintained its optical activity. Similar spectral changes were also observed in the ^{1}H NMR spectra (Figure 3A). The peaks of the original poly-**1**-**H** (a) in its ^{1}H NMR spectrum were rather broad and complicated but became sharper upon complexation with chiral amines in DMSO-d_6−D_2O (9:1, v/v) (b) and D_2O (c) and subsequent removal of the amines. In addition, the aromatic proton resonances of the poly-**1a**-**H** significantly shifted downfield (b), whereas those of the ***h***-poly-**1b**-**H** (c) shifted upfield, indicating intramolecular stacking of the aromatic pendant groups of ***h***-poly-**1b**-**H** in water, which are aligned in a one-handed helical array, thus showing an ICD.[17] The ^{15}N NMR spectra of poly-**1a**-**Me**-^{15}N and ***h***-poly-**1b**-**Me**-^{15}N also showed similar changes, but the changes were not as clear as those observed in the ^{1}H and ^{13}C NMR spectra.

In addition, we recently found that the "as-prepared" poly-**1**-**H** in the absence of chiral amines also very slowly changed

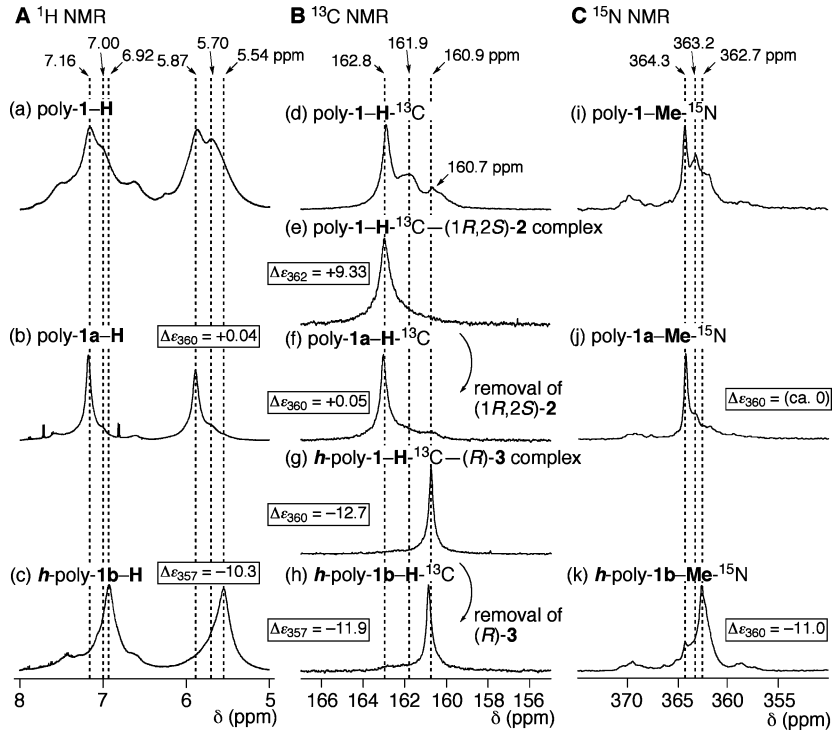

Figure 3. (A) ^{1}H NMR spectra of poly-**1**-**H** (a), poly-**1a**-**H** (run 1 in Table 2) (b), and ***h***-poly-**1b**-**H** (run 2 in Table 2) (c) in D_2O containing 2 mM NaOD at 30 °C. (B) ^{13}C NMR spectra of poly-**1**-**H**-^{13}C before (d) and after helicity induction with (1*R*,2*S*)-**2** in DMSO-d_6−D_2O (9:1, v/v) (run 7 in Table 2) (e) and (*R*)-**3** in D_2O (run 8 in Table 2) (g). The samples had been allowed to stand at 50 °C for 14 (e) and 33 days (g), and their NMR spectra were measured at 30 °C. ^{13}C NMR spectra after removal of the chiral amines measured in D_2O containing 2 mM NaOD at 30 °C are also shown (f and h) (runs 7 and 8 in Table 2). (C) ^{15}N NMR spectra of poly-**1**-**Me**-^{15}N (i), poly-**1a**-**Me**-^{15}N (run 12 in Table 2) (j), and ***h***-poly-**1b**-**Me**-^{15}N (run 13 in Table 2) (k) at 23 °C in $CDCl_3$.

Chart 2. Possible Triad Structures of Polyisocyanides (A), *s-Cis* and *s-Trans* Conformations (B), and Configurational *Syn*−*Anti* Isomerization of Polyisocyanide Dyad (C)

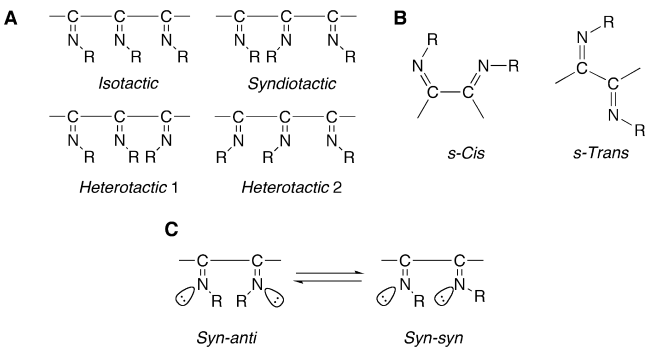

its structure with time at ambient temperature in alkaline water.[17,19] Figure 4 shows the ^{13}C NMR spectra of the main-chain C═N region of poly-**1**-**H**-^{13}C (a) after it had been allowed to stand at ambient temperature for 5 months in D_2O containing 2 mM NaOD (poly-**1′**-**H**-^{13}C (b)); those of poly-**1a**-**H**-^{13}C (c) and ***h***-poly-**1b**-**H**-^{13}C (f) are also shown for comparison. Quite interestingly, the ^{13}C NMR spectrum of poly-**1′**-**H**-^{13}C (b) was almost identical to that of poly-**1a**-**H**-^{13}C (c), showing a sharp signal centered at 162.8 ppm.[22] A similar ^{13}C NMR spectral change took place in ***h***-poly-**1b**-**H**-^{13}C (f) after storing the sample solution at ambient temperature for 2 months (i). On the other hand, upon heating at 80 °C for 2 h, poly-**1a**-**H**-^{13}C (c) and ***h***-poly-**1b**-**H**-^{13}C (f) showed almost the same ^{13}C NMR

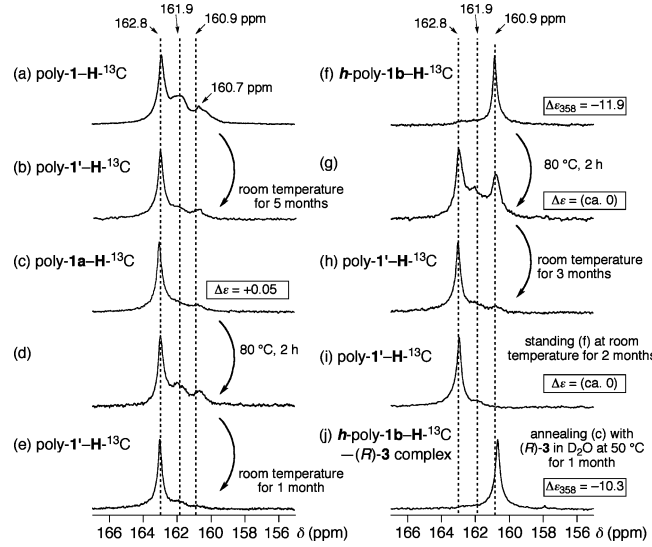

Figure 4. ^{13}C NMR spectra of poly-**1**-**H**-^{13}C (a), poly-**1a**-**H**-^{13}C (run 7 in Table 2) (c), ***h***-poly-**1b**-**H**-^{13}C (run 8 in Table 2) (f), and poly-**1′**-**H**-^{13}C (b and i) obtained from poly-**1**-**H**-^{13}C and ***h***-poly-**1b**-**H**-^{13}C after storing their solutions at room temperature for 5 and 2 months, respectively. ^{13}C NMR spectra (d, e, g, and h) were obtained from poly-**1a**-**H**-^{13}C (c) and ***h***-poly-**1b**-**H**-^{13}C (f) after heating the samples at 80 °C for 2 h (d and g, respectively), followed by storing the samples (d and g) at room temperature for 1 month (e) and 3 months (h), respectively. The ^{13}C NMR spectrum of ***h***-poly-**1b**-**H**-^{13}C—(*R*)-**3** complex obtained from poly-**1a**-**H**-^{13}C after annealing the sample (c) with (*R*)-**3** ([(*R*)-**3**]/[poly-**1a**-**H**-^{13}C] = 10) in D_2O at 50 °C for 1 month is also shown (j). These NMR spectra were measured in D_2O containing 2 mM NaOD at 30 °C.

spectra (d and g, respectively) as that of the "as-prepared" poly-**1**-**H**-^{13}C (a),[17] and the ICD of ***h***-poly-**1b**-**H**-^{13}C completely

(22) Similar changes in the ^{13}C NMR spectra of the main-chain C═N region of poly-**1**-**Me**-^{13}C were also observed (see Figure S6, Supporting Information).

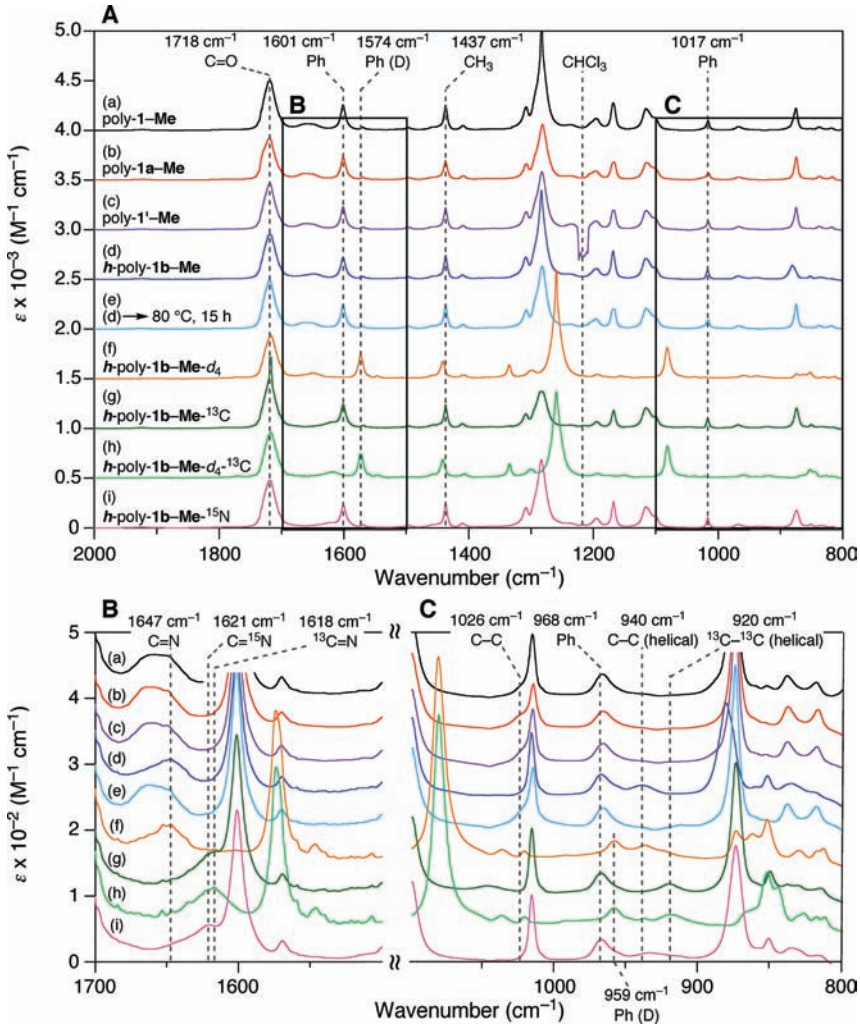

Figure 5. (A) IR spectra of poly-**1**-**Me** (a), poly-**1a**-**Me** (run 1 in Table 2) (b), poly-**1′**-**Me** (c), ***h***-poly-**1b**-**Me** (run 4 in Table 2) (d), ***h***-poly-**1b**-**Me**-d_4 (run 5 in Table 2) (f), ***h***-poly-**1b**-**Me**-^{13}C (run 9 in Table 2) (g), ***h***-poly-**1b**-**Me**-d_4-^{13}C (run 10 in Table 2) (h), and ***h***-poly-**1b**-**Me**-^{15}N (run 13 in Table 2) (i) measured in $CHCl_3$ (800−1150 and 1330−2000 cm^{-1}) and $CDCl_3$ (1150−1330 cm^{-1}) (a, b, d−i) and in $CHCl_3$ (c) at ambient temperature; [polymer] = 50 mg/mL. Poly-**1′**-**Me** (c) was obtained from poly-**1**-**Me** (a) after storing its $CHCl_3$ solution at room temperature for 12 days. The IR spectrum after heating the $CHCl_3$ solution of ***h***-poly-**1b**-**Me** (d) at 80 °C for 15 h is also shown (e). Magnified IR spectra corresponding to the areas indicated by the squares in panel A are shown in panels B and C.

disappeared. Further storage of the samples (d and g) at room temperature for 1 month (poly-**1′**-**H**-^{13}C (e)) and 3 months (poly-**1′**-**H**-^{13}C (h)) produced significant changes in their ^{13}C NMR spectra, showing a sharp signal centered at 162.8 ppm. These results revealed that poly-**1′**-**H** and poly-**1a**-**H** may have the thermodynamically most favorable structure, and such a structural change will slowly take place via configurational isomerization around the C═N double bonds in solution. A similar change in the structure, accompanied by a preferred-handed helicity induction, appears to occur slowly under predominantly thermodynamic control in the "as-prepared" poly-**1**-**H** during the complexation with chiral amines in DMSO,[19] although the optical activity due to the excess one helical sense is tentative and instantly disappears after removal of the chiral amines (poly-**1a**-**H**),[17,20] suggesting that this helicity induction process in DMSO involves a helical conformational change. Interestingly, the thermodynamically most stable poly-**1a**-**H** further changed its structure into a preferred-handed helical polymer with a macromolecular helicity memory (***h***-poly-**1b**-**H**) upon complexation with chiral amines in water (j). As a consequence, the polyisocyanides with different main-chain structures, poly-**1**-**H**, poly-**1a**-**H**, and ***h***-poly-**1b**-**H**, can interconvert into each other as revealed by the NMR studies.[23]

IR and VCD Studies. Additional evidence of the main-chain structural changes during the helicity induction in poly-**1**-**H** as well as its one-handed helical structure was obtained from the IR and VCD spectra. A problem in any approach based on analyzing vibrational spectra is the difficulty in resolving the contributions from individual residues. To this end, a series of isotopically labeled poly-**1**-**H**'s with D, ^{13}C, or ^{15}N before and after the helicity induction with chiral amines in different solvents and after removal of the chiral amines were prepared and esterified with CH_2N_2 (Table 2), and these polymers were used to assign the peaks in the vibrational spectra.

Figure 5 shows the IR spectra of poly-**1**-**Me**, poly-**1a**-**Me**, poly-**1′**-**Me**, ***h***-poly-**1b**-**Me**, and the isotopically labeled ***h***-poly-**1b**-**Me**-d_4, ***h***-poly-**1b**-**Me**-^{13}C, ***h***-poly-**1b**-**Me**-d_4-^{13}C, and ***h***-poly-**1b**-**Me**-^{15}N measured in $CHCl_3$ or $CDCl_3$. Noticeable changes in the IR spectra after helicity induction and memory were

(23) A similar dynamic helical model has also been proposed by Cornelissen, Nolte, and co-workers for helical poly(isocyanopeptide)s derived from β-amino acids. See ref 10e.

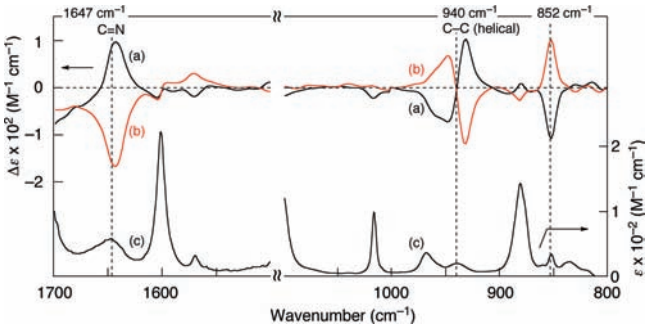

Figure 6. VCD (a, b) and IR (c) spectra of ***h***-poly-**1b**-**Me** prepared by (*R*)-**3** (run 4 in Table 2) (a, c) and (*S*)-**3** (run 3 in Table 2) (b), measured in $CHCl_3$ at ambient temperature ([polymer] = 120 (a, b) and 50 mg/mL (c)).

observed in the C═N stretching and the main-chain C−C vibration regions (a and d in Figure 5B,C). The C═N stretching (1647 cm^{-1}) and the main-chain helical C−C vibrations (940 cm^{-1}) of ***h***-poly-**1b**-**Me** observed in its IR spectrum were significantly different from those of poly-**1**-**Me**, poly-**1a**-**Me**, and poly-**1′**-**Me** (a−c in Figure 5B). The former band was shifted to lower wavenumbers by ca. 30 cm^{-1} relative to the original poly-**1**-**Me**, poly-**1a**-**Me**, and poly-**1′**-**Me**, and the latter band appeared as a new band after the helix induction and memory. These bands are characteristic for the helical polyisocyanide because ***h***-poly-**1b**-**Me** showed distinct Cotton effects in the C═N stretching region as well as the main-chain C−C bond vibration region in its VCD spectrum (see Figure 6). These assignments were supported by the facts that the C═N stretching vibrations were shifted to lower wavenumbers by ca. 30 cm^{-1} relative to that of ***h***-poly-**1b**-**Me** in the IR spectra of ***h***-poly-**1b**-**Me**-^{13}C, ***h***-poly-**1b**-**Me**-d_4-^{13}C, and ***h***-poly-**1b**-**Me**-^{15}N (g−i in Figure 5B), and that the main-chain C−C vibration at 940 cm^{-1} observed in the IR spectrum of ***h***-poly-**1b**-**Me** was significantly shifted to lower wavenumbers when the carbon or nitrogen of the C═N double bonds was labeled with ^{13}C (***h***-poly-**1b**-**Me**-^{13}C and ***h***-poly-**1b**-**Me**-d_4-^{13}C) or ^{15}N (***h***-poly-**1b**-**Me**-^{15}N) (g−i in Figure 5C). In addition, poly-**1**-**Me**, poly-**1a**-**Me**, and poly-**1′**-**Me** have an additional weak but apparent shoulder peak around 1026 cm^{-1}. It seems likely that the shoulder peak almost completely disappeared after the helicity induction and memory in water (***h***-poly-**1b**-**Me**), accompanied by appearance of the main-chain C−C bond vibration at 940 cm^{-1} (a−d in Figure 5C). This shoulder peak was assigned to a type of C−C bond vibration, since after enrichment with ^{13}C (poly-**1**-**Me**-^{13}C) the peak disappeared (e in Figure S7, Supporting Information). These assignments were further supported by the fact that the typical peaks at 1647 and 940 cm^{-1} for ***h***-poly-**1b**-**Me** disappeared after heating the sample at 80 °C for 15 h (d and e in Figure 5); the resulting IR spectrum was almost identical to that of poly-**1**-**Me** (a and e in Figure 5). We noted that poly-**1a**-**Me** and poly-**1′**-**Me** showed almost identical IR spectra, as expected from the NMR results. These IR results revealed a configurational isomerization around the C═N double bonds that surely takes place during the helicity induction and memory; that is, an imino configurational mixture of *syn* and *anti* forms of the original poly-**1** is transformed into an excess of a single configuration upon complexation with the chiral amines.

The VCD spectra of ***h***-poly-**1b**-**Me** and the isotopically labeled polymers (Figures 6 and S8 (Supporting Information)) provided strong evidence of a one-handed helical structure of the polyisocyanides. The enantiomeric helical ***h***-poly-**1b**-**Me**'s obtained from the corresponding ***h***-poly-**1b**-**H**'s induced by (*R*)- and (*S*)-**3** showed virtually mirror-image Cotton effects in the C═N stretching and the main-chain C−C vibration regions in their VCD spectra (Figure 6).[17] In addition, ***h***-poly-**1b**-**Me**'s exhibited an intense split-type Cotton effect in the main-chain C−C bond vibration region around 940 cm^{-1}, a characteristic band for the helical polyisocyanides as mentioned above, and the positive and negative VCD signals go through near the absorption maximum of the C−C bond vibration. Another clear VCD was also observed at 852 cm^{-1}, which may provide additional structural information about the helical structure of ***h***-poly-**1b**-**Me**, but peak assignment was difficult due to the complexity of its vibrational mode, even though the labeled polymers were used for their assignments. The isotopically labeled helical polyisocyanides also showed virtually identical VCD spectral patterns in the C═N stretching and C−C bond vibration regions (Figure S8).

The advantages of VCD are not only its sensitivity for chiral nonchromophoric molecules, but also reliable theoretical calculations of its spectrum using methods available in the Gaussian program.[24] Taking advantage of the available calculation method, calculations of poly(phenyl isocyanide) (PPI), a model polymer of the helical ***h***-poly-**1b**-**Me**, were then performed to simulate its VCD spectrum, which was further used to determine the helix-sense (right- or left-handed helix) of ***h***-poly-**1b**-**Me** by comparison with the experimental VCD spectra (see below).

Persistence Length Measurements. We next estimated the backbone stiffness (persistence length *q*) of HMW-poly-**1**-**Me**, HMW-poly-**1a**-**Me**, and HMW-***h***-poly-**1b**-**Me** in $CHCl_3$.[25] The *q* values of these polymers were estimated using SEC equipped with multiangle laser light scattering (MALS) and refractive index detectors in series along with the wormlike chain model.[26] This model can be described as an analytical function of the molecular weight (M_w) and the radius of gyration (*S*) if the *q* values and the molar mass per unit contour length (M_L), which eventually leads to the monomer unit height (*h*), are given. In this way, the dependences of the M_w on the radii of gyration of these polymers were explored by using the SEC-MALS system and $CHCl_3$ as the eluent (Figure 7). The solid curves in the plots were calculated using the parameters determined from the

(24) Frisch, M. J.; et al. *Gaussian 03*, Revision C.02; Gaussian, Inc.: Wallingford, CT, 2004.
(25) The persistence length (*q*) is a useful measure to evaluate the stiffness of rodlike polymers, but only a limited number of *q* values have been determined for synthetic helical polymers. See: (a) Sato, T.; Teramoto, A. *Adv. Polym. Sci.* **1996**, *126*, 85–161. (b) Nieh, M.-P.; Goodwin, A. A.; Stewart, J. R.; Novak, B. M.; Hoagland, D. A. *Macromolecules* **1998**, *31*, 3151–3154. (c) Gu, H.; Nakamura, Y.; Sato, T.; Teramoto, A.; Green, M. M.; Andreola, C. *Polymer* **1999**, *40*, 849–856. (d) Teramoto, A.; Terao, K.; Terao, Y.; Nakamura, N.; Sato, T.; Fujiki, M. *J. Am. Chem. Soc.* **2001**, *123*, 12303–12310. (e) Nomura, R.; Tabei, J.; Nishiura, S.; Masuda, T. *Macromolecules* **2003**, *36*, 561–564. (f) Ashida, Y.; Sato, T.; Morino, K.; Maeda, K.; Okamoto, Y.; Yashima, E. *Macromolecules* **2003**, *36*, 3345–3350. (g) Okoshi, K.; Sakajiri, K.; Kumaki, J.; Yashima, E. *Macromolecules* **2005**, *38*, 4061–4064. (h) Okoshi, K.; Sakurai, S.-i.; Ohsawa, S.; Kumaki, J.; Yashima, E. *Angew. Chem., Int. Ed.* **2006**, *45*, 8173–8176. Persistence length values of certain polyisocyanide derivatives have been measured. See ref 11 and the following: (i) Bieglé, A.; Mathis, A.; Galin, J.-C. *Macromol. Chem. Phys.* **2000**, *201*, 113–125. (j) Samorí, P.; Ecker, C.; Gössl, I.; de Witte, P. A. J.; Cornelissen, J. J. L. M.; Metselaar, G. A.; Otten, M. B. J.; Rowan, A. E.; Nolte, R. J. M.; Rabe, J. P. *Macromolecules* **2002**, *35*, 5290–5294. (k) Okoshi, K.; Nagai, K.; Kajitani, T.; Sakurai, S.-i.; Yashima, E. *Macromolecules* **2008**, *41*, 7752–7754.
(26) (a) Yamakawa, H.; Fujii, M. *Macromolecules* **1974**, *7*, 128–135. (b) Yamakawa, H.; Yoshizaki, T. *Macromolecules* **1980**, *13*, 633–643.

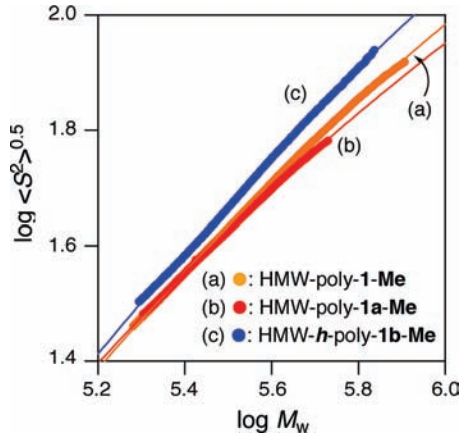

Figure 7. Double-logarithmic plots of the radius of gyration versus the molecular weight of HMW-poly-**1**-**Me** (a), HMW-poly-**1a**-**Me** (run 14 in Table 2) (b), and HMW-***h***-poly-**1b**-**Me** (run 16 in Table 2) (c) in $CHCl_3$ obtained by SEC-MALS measurements at 25 °C. Solid curves were obtained on the basis of the wormlike chain theory and fit well with the experimental data. The evaluated parameters are as follows: HMW-poly-**1**-**Me**, $q = 59$ nm, $M_L = 1618$ nm^{-1}, $h = 0.10$ nm; HMW-poly-**1a**-**Me**, $q = 43$ nm, $M_L = 1483$ nm^{-1}, $h = 0.11$ nm; HMW-***h***-poly-**1b**-**Me**, $q = 88$ nm, $M_L = 1592$ nm^{-1}, $h = 0.10$ nm.

fits of the unperturbed wormlike chain model over the entire M_w studied range and are represented by the theoretical values of $\langle S^2 \rangle^{0.5}$.

The calculated q value of the "as-prepared" HMW-poly-**1**-**Me** is 59 nm, which is slightly smaller than that of a helical polyisocyanopeptide (76 nm).[25j] Interestingly, HMW-***h***-poly-**1b**-**Me** (run 16 in Table 2) with a macromolecular helicity memory exhibited the significantly higher q value of 88 nm. In contrast, HMW-poly-**1a**-**Me** (run 14 in Table 2), which lost optically activity after helicity induction, showed a dramatic decrease in its q value to 43 nm, leading to a rather semirigid polymer. These changes in the q values clearly demonstrate the specific configurational isomerization around the C=N double bonds (*syn*−*anti* isomerization) that likely takes place during the helicity induction process, resulting in the changes of the main-chain stiffness of HMW-poly-**1**-**Me**.

Helical Structures. Although the helical structure of polyisocyanides has been postulated to be a 4-unit/1-turn (4/1) helical conformation on the basis of the X-ray analysis of poly(α-phenylethyl isocyanide) (PPEI)[2b,d,4a] due to using unoriented samples, the exact helical structure was difficult to determine on the basis of their X-ray diffractions. Nolte and co-workers successfully synthesized a series of rigid-rod helical polyisocyanopeptides with a controlled helicity, some of which showed cholesteric LC phases.[10a,b,e,g] X-ray diffractions of their unoriented cast films were then measured, but only an orthorhombic arrangement of the polymers in the solid could be proposed.[10b]

Recently, we found that some helical poly(phenyl isocyanide)s derived from low-molecular-weight ***h***-poly-**1b**-**H** ($M_n = 3.3 \times 10^4$) after modification of the carboxy pendant groups with bulky primary and secondary amines or primary amines with a long ethylene oxide trimer or a pyridylmethyl group formed lyotropic LC phases in concentrated solutions due to their main-chain stiffness, thus showing a fingerprint texture.[18] In contrast, the original ***h***-poly-**1b**-**H** and ***h***-poly-**1b**-**Me** did not show LC phases in concentrated solutions. However, as we anticipated, HMW-poly-**1**-**H** was found to form a nematic LC phase in concentrated alkaline water solution (15−20 wt %), thus showing a clear Schlieren texture (Figure 8A). Its methyl

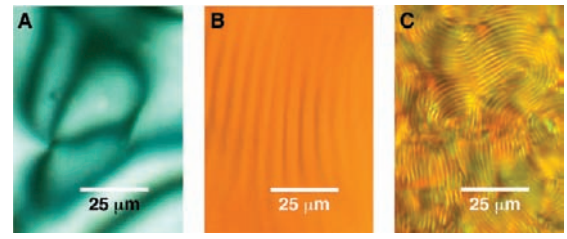

Figure 8. Polarized optical micrographs of LC phases of nematic HMW-poly-**1**-**H** (run 6 in Table 1) (A) and cholesteric HMW-***h***-poly-**1b**-**H** (run 15 in Table 2) (B) in alkaline water and HMW-***h***-poly-**1b**-**Me** (run 15 in Table 2) (C) in 1,1,2,2-tetrachloroethane. Concentrations of the polymers (A−C) were 20, 15, and 20 wt %, respectively.

ester (HMW-poly-**1**-**Me**) also showed a nematic LC phase in $CHCl_3$. Furthermore, the corresponding helical polymers, HMW-***h***-poly-**1b**-**H** and HMW-***h***-poly-**1b**-**Me**, exhibited cholesteric LC phases in alkaline water (15 wt %) and 1,1,2,2-tetrachloroethane (20 wt %), respectively, showing a fingerprint texture (B and C in Figure 8, respectively). The spacings of the fringes corresponding to the half-pitch of the cholesteric helical structure were 6.0 (B) and 1.8 μm (C), respectively. This finding of nematic and cholesteric LC formations of the polyisocyanides before and after the helicity induction and memory makes possible the analysis of their helical structures by XRD, because we can make shear-oriented films from the LC samples.[10h,27]

Figure 9B shows the wide-angle X-ray diffraction (WAXD) pattern with different sensitivity ranges of the uniaxially oriented HMW-***h***-poly-**1b**-**Me** film prepared from its concentrated cholesteric LC $CHCl_3$ solution. The oriented HMW-***h***-poly-**1b**-**Me** film showed broad but apparent equatorial and near-meridional reflections. The five equatorial reflections, 14.19, 10.56, 6.46, 5.13, and 4.03 Å, can be indexed with a simple two-dimensional tetragonal lattice of $a = 14.37$ Å (Table S1, Supporting Information). Next, we determined the fiber period to be 10.30 Å ($= c$) from the layer lines (1/10.30 Å^{-1} apart) attributed to the helical structure, where the weak meridional reflection of nearly 4.1 Å was excluded from this analysis because the reflection cannot be assumed for the regular helical structure of HMW-***h***-poly-**1b**-**Me**, as described below for HMW-poly-**1**-**Me**. The observed density (1.259 g/cm^3) indicates that this unit cell includes 10 monomer units/1 chain along the c-axis, in agreement with the calculated density (1.258 g/cm^3).[28] Although we could not observe a meridian reflection on the 10th layer line (1.03 Å) (see Table S1) corresponding to the unit height (h) of the helical structure, even when the X-ray measurements were performed using a cylindrical camera with the samples tilted ca. 48° normal to the beam, the most plausible helical structure of the HMW-***h***-poly-**1b**-**Me** is proposed to be a 10-unit/3-turn helix (10/3) (Figure 10A) on the basis of the strong reflection on the third layer line (3.41 Å) and the reflection on the fourth layer line (nearly 2.6 Å), which

(27) (a) Nagai, K.; Sakajiri, K.; Maeda, K.; Okoshi, K.; Sato, T.; Yashima, E. *Macromolecules* **2006**, *39*, 5371–5380. (b) Sakurai, S.-i.; Okoshi, K.; Kumaki, J.; Yashima, E. *Angew. Chem., Int. Ed.* **2006**, *45*, 1245–1248. (c) Sakurai, S.-i.; Ohsawa, S.; Nagai, K.; Okoshi, K.; Kumaki, J.; Yashima, E. *Angew. Chem., Int. Ed.* **2007**, *46*, 7605–7608.

(28) The densities of the HMW-poly-**1**-**Me**, HMW-poly-**1a**-**Me**, and HMW-***h***-poly-**1b**-**Me** films were measured by the standard flotation method in a KBr saturated aqueous solution−water mixture at ambient temperature (20−25 °C).

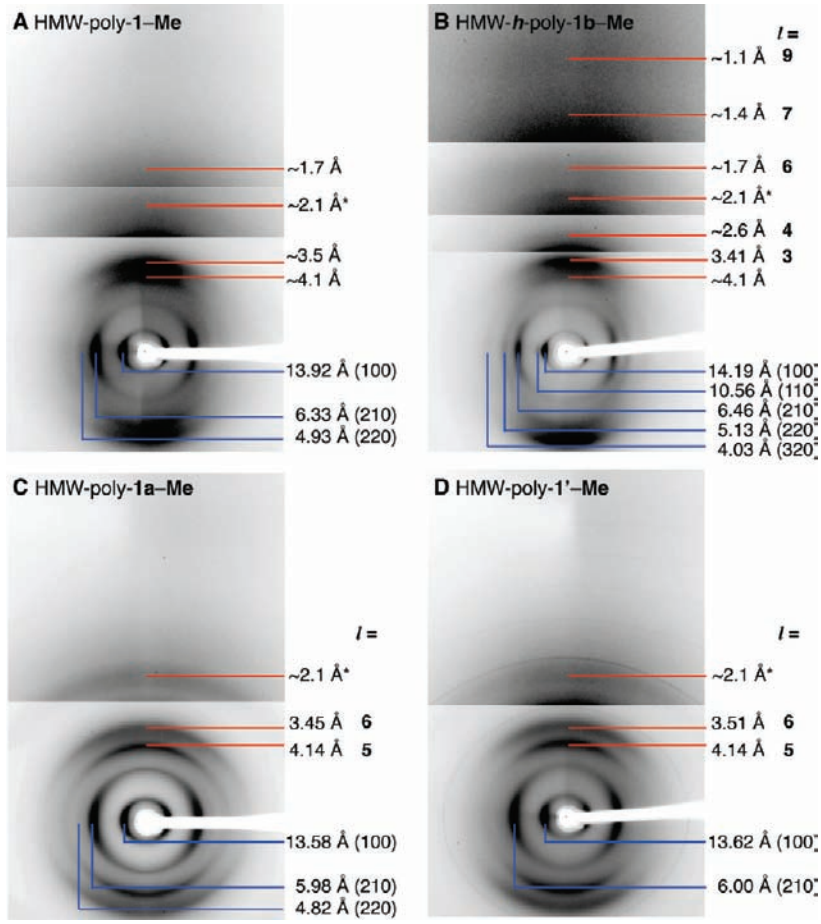

Figure 9. X-ray diffraction patterns of oriented films obtained from optically inactive HMW-poly-**1**-**Me** (A), optically active HMW-***h***-poly-**1b**-**Me** with helicity memory (run 16 in Table 2) (B), optically inactive HMW-poly-**1a**-**Me** (run 14 in Table 2) (C), and HMW-poly-**1′**-**Me** (D) with different ranges of sensitivities taken from the edge-view position with a beam parallel to the film surface using a curved imaging plate; the vertical direction nearly corresponds to the helical axis. HMW-poly-**1′**-**Me** was obtained from HMW-poly-**1**-**Me** after its $CHCl_3$ solution was stored at room temperature for 3 months. The representative layer lines and the main reflections are labeled. The reflections around 2.1 Å indicated by asterisks are probably not attributed to the reflections due to helical structures judging from WAXD measurements of the same polymer films using a flat imaging plate (see Figure S9, Supporting Information).

correspond to the first- or second-order Bessel functions, respectively (Table S1), consistent with the helical diffraction theory.[29]

Next, we tried to elucidate the structures of HMW-poly-**1a**-**Me** and HMW-poly-**1′**-**Me**, which were anticipated to be the same on the basis of their essentially identical NMR and IR spectra, by XRD in the same way in order to address the questions concerning a difference in the helical structures of the polyisocyanides induced in DMSO and water in the presence of chiral amines, and why the preferred-handed helical structure induced in DMSO cannot be memorized after removal of the chiral amines. The XRD data of the oriented optically inactive HMW-poly-**1a**-**Me** film indicated that the polymer chains are packed with a smaller tetragonal lattice of $a = 13.56$ Å (Figure 9C and Table S1). A clearly strong and sharp reflection of 4.14 Å, which was also observed in the HMW-***h***-poly-**1b**-**Me** film as a weak reflection (Figure 9B), suggests that the HMW-poly-**1a**-**Me** may have another regular helical structure, different from the 10/3 helical structure proposed for HMW-***h***-poly-**1b**-**Me**. This speculation is supported by the IR and NMR results; poly-**1a**-**Me** and ***h***-poly-**1b**-**Me** exhibited rather sharp proton and carbon resonances with different chemical shifts in their NMR spectra (Figures 3 and S6), and the IR spectrum of poly-**1a**-**Me** is significantly different from that of ***h***-poly-**1b**-**Me**, particularly in the C═N stretching and the main-chain C−C bond vibration regions (Figure 5). As expected, the thermodynamically most stable HMW-poly-**1′**-**Me** showed an XRD pattern almost identical to that of HMW-poly-**1a**-**Me**. We first determined the fiber period to be 20.70 Å ($= c$) from the layer lines (1/20.70 $Å^{-1}$ apart) attributed to the helical structure. The observed density (1.255 g/cm^3) indicates that this unit cell includes 18 monomer units/1 chain along the *c*-axis, in agreement with the calculated density (1.266 g/cm^3).[28] Although the number of meridian reflections is limited, the structure of poly-**1a**-**Me** and poly-**1′**-**Me** could be proposed to be an 18-unit/5-turn helix (18/5) on the basis of the strong reflections on the fifth layer line (4.14 Å) and the sixth layer line (3.45 Å) (Table S1). However, we assumed that the structure of poly-**1a**-**Me** and poly-**1′**-**Me** may be different from an *s-cis*-isotactic structure like ***h***-poly-**1b**-**Me** because of the essentially different IR and NMR spectral patterns from those of ***h***-poly-**1b**-**Me**. Poly-**1a**-**Me** and poly-**1′**-**Me** most likely take the thermodynamically most stable structures. We then performed molecular mechanics (MM) calculations (see the Supporting Information) in order to obtain the optimized helical structure

(29) Cochran, W.; Crick, F. H. C.; Vand, V. *Acta Crystallogr.* **1956**, *5*, 581–586.

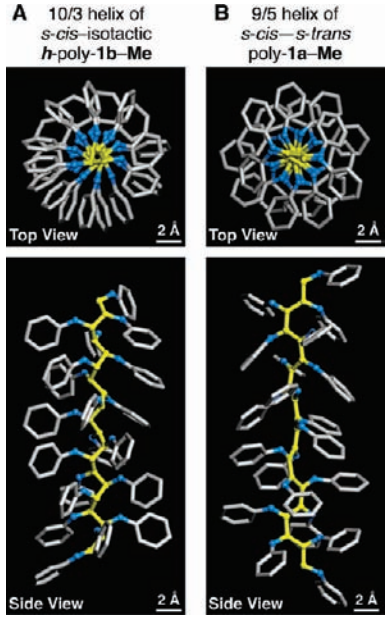

Figure 10. Top and side views of a 10/3 right-handed helical structure of *s-cis*-isotactic ***h***-poly-**1b**-**Me** (20-mer) (A) and a 9/5 right-handed helical structure of *s-cis—s-trans* poly-**1a**-**Me** (20-mer) with two monomer units having alternative *s-cis* and *s-trans* conformations as a repeating unit (B). The main-chain carbon and nitrogen atoms are shown in yellow and blue, respectively, using the ball-and-stick model for clarity. The phenyl groups of the side chains are shown in gray using the cylinder model, and hydrogen atoms and the methyl ester groups are omitted for clarity.

for poly-**1a**-**Me** and poly-**1′**-**Me** that satisfies the 18/5 helix; the optimized 18/5 helical structure was found to alternate *s-cis* and *s-trans* (Figure 10B) and thus can be regarded as a 9/5 helix with two continuous *s-cis* and *s-trans* monomer units as a repeating unit.[30,31] A similar helical polyisocyanide structure was theoretically proposed by Clericuzio and Salvadori.[14a]

The structural determination for HMW-poly-**1**-**Me** was also attempted using the same strategy as for the HMW-***h***-poly-**1b**-**Me** and HMW-poly-**1a**-**Me**, measuring the WAXD of an oriented optically inactive HMW-poly-**1**-**Me** film prepared from a concentrated nematic LC $CHCl_3$ solution (Figure 9A). The XRD data indicate that the HMW-poly-**1**-**Me** chains are packed with a slightly smaller tetragonal lattice of $a = 13.96$ Å (Table S1). However, we could not detect the reflection of nearly 2.6 Å, corresponding to the fourth layer line of the 10/3 helical structure as observed for HMW-***h***-poly-**1b**-**Me**, which suggests that there is no correlation with the long-range order as observed for the HMW-***h***-poly-**1b**-**Me**. The remaining third layer line of the 10/3 helix indicates that some poly-**1**-**Me** segments may form nearly 10/3 helices having an average helical pitch of nearly 3.5 Å, but it is postulated that other HMW-poly-**1**-**Me** segments likely form another helical structure corresponding to that of HMW-poly-**1a**-**Me**, that is, a nearly 9/5 helical structure with two monomer units as the repeating unit because of a diffuse but relatively strong meridional reflection of nearly 4.1 Å, which may correspond to the fifth layer line of the 9/5 helical structure, as observed for the HMW-poly-**1a**-**Me**. The intensity of this reflection is definitely strong for the stereoirregular HMW-poly-**1**-**Me** but weak for the regular HMW-***h***-poly-**1b**-**Me** (Figure 9B). These observations are quite consistent with the IR and NMR results. In addition, there results imply that the regularity of the helical backbone of HMW-***h***-poly-**1b**-**Me** is still imperfect and the reflection in the region of nearly 4.1 Å for HMW-***h***-poly-**1b**-**Me** will disappear when the regularity of the helical backbone increases.

Consequently, the ***h***-poly-**1b**-**Me** backbone, with a preferred-handed helical conformation, consists of the regular 10/3 helix as the major structural element, and the poly-**1a**-**Me** and poly-**1′**-**Me** chains have predominantly 9/5 helices with two monomer units as a repeating unit whose helical structure appears to be completely different from that of the ***h***-poly-**1b**-**Me** with respect to their main-chain conformations and configurations. The poly-**1**-**Me** chains may be composed mainly of a mixture of a nearly 10/3 helix, a nearly 9/5 helix, and some other disordered segments.

Computational Studies on Helical Structure. To gain further information regarding the helical structure of ***h***-poly-**1b**, PPI oligomers with a forced periodic structure were employed as a model polymer, and their structures were calculated according to a procedure developed by Sawabe and co-workers which is useful for calculating the structure and its related property of a periodic polymer based on a small sized oligomer (see the Supporting Information).[32] Calculations were performed using the semiempirical PM3 method[33] and the hybrid density functional theory (DFT) method at the B3LYP level.[34−37] A mixed basis set (MIX), consisting of the 6-31G(d) basis[38,39] for nitrogen and carbon atoms of the main-chain and the 6-31G basis[39] for other atoms, was used. All calculations were carried out using Gaussian 03.[24]

At the PM3 level, we performed the full optimization for the *s-cis*-isotactic PPIs of 4-, 10-, 20-, 30-, and 40-mers. The increase in the main-chain length led to the convergence of the dihedral angle ($C_1-C_2-C_3-C_4$) of the central part of the oligomers along the main-chain to 80°. On the basis of the converged structure, the repeating structure unit was confirmed to be a monomer (>C═N−Ph) for the *s-cis* isotactic PPI. A similar procedure was performed for the *s-trans* isotactic PPI, and its repeating structure unit for the periodicity was found to be two monomers.

At the B3LYP/MIX level, geometry optimizations for the *n*-mer ($n = 1-14$) oligomers of the *s-cis* isotactic PPI were then carried out under the forced periodic condition (see the

(30) The MM calculations of the *s-cis*-isotactic 18/5 helical structure of poly-**1a**-**Me** and poly-**1′**-**Me** with a repeating structure unit (1-mer) for the periodicity like ***h***-poly-**1b**-**Me** revealed that the energy-minimized conformation had a much higher energy than the 10/3 helical ***h***-poly-**1b**-**Me**. We then considered a plausible helical structure of poly-**1a**-**Me** and poly-**1′**-**Me** that has a repeating structure unit (2-mer) for the periodicity (Chart S3, Supporting Information) and found that the energy-minimized 9/5 helical structure with an alternating *s-cis* and *s-trans* conformation had a much lower energy than ***h***-poly-**1b**-**Me** (see the Supporting Information).

(31) Although the IR and NMR spectral results suggest that the main-chain configuration of poly-**1a**-**Me** may differ from that of ***h***-poly-**1b**-**Me** (Figures 3 and S6), the optimized helical structure of poly-**1a**-**Me** obtained by the empirical MM calculations appears to be isotactic; a syndiotactic structure may likely be more plausible for poly-**1a**-**Me** to explain the differences in their IR and NMR spectra. Apparently, more detailed nonempirical calculations are required to determine the main-chain configuration of poly-**1a**-**Me**.

(32) Ochi, N.; Hase, Y.; Maeda, K.; Yashima, E.; Sawabe, K. Manuscript in preparation.
(33) Stewart, J. J. P. *J. Comput. Chem.* **1989**, *10*, 209–220.
(34) Becke, A. D. *Phys. Rev. A* **1988**, *38*, 3098–3100.
(35) Becke, A. D. *J. Chem. Phys.* **1993**, *98*, 5648–5642.
(36) Lee, C.; Yang, W.; Parr, R. G. *Phys. Rev. B* **1988**, *37*, 785–789.
(37) Stephens, P. J.; Devlin, J. F.; Chabalowski, C. F.; Frisch, M. J. *J. Phys. Chem.* **1994**, *98*, 11623–11627.
(38) Hehre, W. J.; Ditchfield, R.; Pople, J. A. *J. Chem. Phys.* **1972**, *56*, 2257–2261.
(39) Hariharan, P. C.; Pople, J. A. *Theor. Chim. Acta.* **1973**, *28*, 213–222.

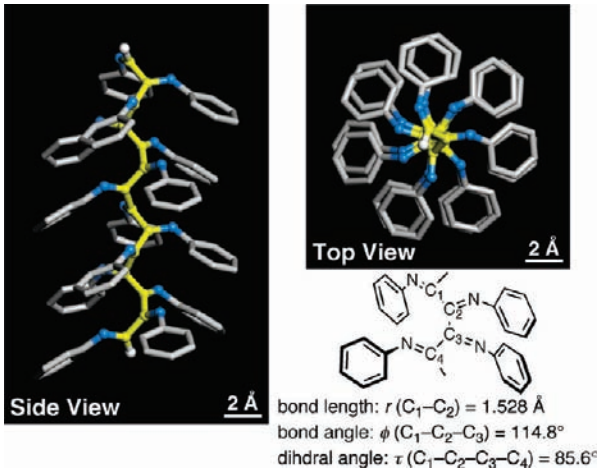

Figure 11. Top and side views of the optimized 7/2 right-handed helical structure of *s-cis* isotactic PPI (14-mer). The main-chain carbon and nitrogen atoms are shown in yellow and blue, respectively, using the ball-and-stick model for clarity. The phenyl groups of the side chains are shown in gray using the cylinder model, and hydrogen atoms are omitted for clarity.

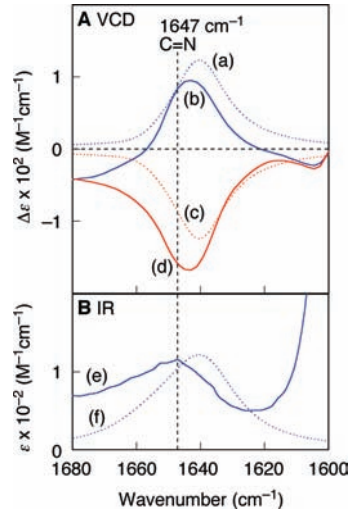

Figure 12. Comparison between calculated and observed IR and VCD spectra. (A) VCD spectra of ***h***-poly-**1b**-**Me** prepared by (*R*)-**3** (run 4 in Table 2) (b) and (*S*)-**3** (run 3 in Table 2) (d), measured in $CHCl_3$ at ambient temperature ([polymer] = 120 mg/mL), and the calculated left-handed (a) and right-handed helical PPIs (c). (B) IR spectra of ***h***-poly-**1b**-**Me** prepared by (*R*)-**3** (run 4 in Table 2) (e) measured in $CHCl_3$ at ambient temperature and the calculated left-handed helical PPI (f). The calculated IR and VCD spectra were constructed from calculated dipole and rotational strengths assuming Lorentzian band shape with a half-width at half-maximum of 3 cm^{-1}. The calculated frequencies were scaled by a frequency-independent factor of 0.9614.[44]

Supporting Information). As a result, the 14-mer helical PPI was sufficient to yield the physical and chemical properties of the true periodic polymer. The optimized *s-cis* isotactic PPI has a repeating structure unit (1-mer) for the periodicity and a helical conformation with the bond length (C_1-C_2, 1.528 Å), the bond angle ($C_1-C_2-C_3$, 114.8°), and the dihedral angle ($C_1-C_2-C_3-C_4$, 85.6°), giving a 7-unit/2-turn (7/2) helix (see Figure 11 for a 7/2 right-handed helical structure of PPI). For comparison, the 10/3 right-handed helical structure of ***h***-poly-**1b**-**Me** postulated by the X-ray analysis is shown in Figure 10A; the pendant methyl ester groups were omitted for clarity. The calculated helical structure of PPI (7/2 helix) appears to be analogous to that of a PPI derivative, ***h***-poly-**1b**-**Me** (10/3 helix) experimentally determined by XRD measurements; the difference in their helical structures (7/2 versus 10/3 helix) may be attributed to the difference in their pendant structures.[40]

The IR and VCD spectra for the optimized 7/2 helical PPI (14-mer) were then calculated at the B3LYP/MIX level. We noted that the observed and calculated IR and VCD[41] spectra in the main-chain C═N stretching vibration regions were in excellent agreement with each other (Figure 12).[42] The calculated VCD spectra for the left- and right-handed helical 7/2 PPIs (a and c in Figure 12, respectively) were then compared with the experimental spectra of the helical ***h***-poly-**1b**-**Me**'s showing positive and negative Cotton effect signs (b and d in Figure 12A, respectively), revealing that the helical ***h***-poly-**1b**-**Me**, showing a negative Cotton effect in the main-chain C═N stretching vibration region, has a right-handed helix. This assignment of the helical sense in the poly(phenyl isocyanide)s agrees with those determined by the exciton-coupled CD method[43] and by the direct atomic force microscopy (AFM) observations of the self-assembled helical poly(phenyl isocyanide) derivatives.[10d,h]

Mechanism of Helicity Induction and Memory. Combining the present experimental observations, theoretical calculations, and persistence length measurements allowed us to propose the mechanism of helix induction in poly-**1**-**H** with chiral amines in DMSO and water and the subsequent memory of the macromolecular helicity in water, as well as possible structures of the relevant polyisocyanides (Figure 13).

The "as-prepared" poly-**1**-**H** may be composed of a mixture of a nearly 10/3 helix and a nearly 9/5 helix, with two monomer units as a repeating unit as well as disordered segments arising from the *syn* and *anti* states of each monomer unit, as indicated by the IR and NMR results, lacking a long-range order in its structure. In the presence of chiral amines in water or aqueous organic solutions containing more than 50 vol % water, the poly-**1**-**H** folds into a rigid preferred-handed 10/3 helical structure accompanied by transformation of an imino configurational mixture of *syn*- and *anti*-poly-**1**-**H** to one of a single configuration, and this selective configurational isomerization, assisted by hydrophobic and chiral ionic interactions in water, forces the helical conformation on the polymer backbone to take an excess helical sense. Therefore, the induced helix is supposed to be kinetically controlled and remains after removal of the chiral amines at ambient temperature, while at high temperature the helical conformation unravels due to the *syn*−*anti* configu-

(40) The optimized *s-trans* isotactic PPI has a 5/2 helix with two monomer units as a repeating unit for the periodicity (see Figure S2 and the Supporting Information). The result also proves the validity of the assigned *s-cis* isotactic helical structure of ***h***-poly-**1b**-**Me**.

(41) Cheeseman, J. R.; Frisch, M. J.; Devlin, F. J.; Stephens, P. J. *Chem. Phys. Lett.* **1996**, *252*, 211–220.

(42) Because PPI and ***h***-poly-**1b**-**Me** possess different pendant groups, the calculated IR and VCD of PPI in other vibration regions were not in agreement with the observed IR and VCD spectra of ***h***-poly-**1b**-**Me**.

(43) (a) Takei, F.; Hayashi, H.; Onitsuka, K.; Kobayashi, N.; Takahashi, S. *Angew. Chem., Int. Ed.* **2001**, *40*, 4092–4094. The helical sense of a one-handed helical polyguanidine is also assigned on the basis of its observed and calculated VCD spectra; see ref 3b. For other examples of helical sense assignments of polyisocyanides, see ref 7 and the following: (b) Cornelissen, J. J. L. M.; Sommerdijk, N. A. J. M.; Nolte, R. J. M. *Macromol. Chem. Phys.* **2002**, *203*, 1625–1630.

(44) Merrick, J. P.; Moran, D; Radom, L. *J. Phys. Chem. A* **2007**, *111*, 11683–11700.

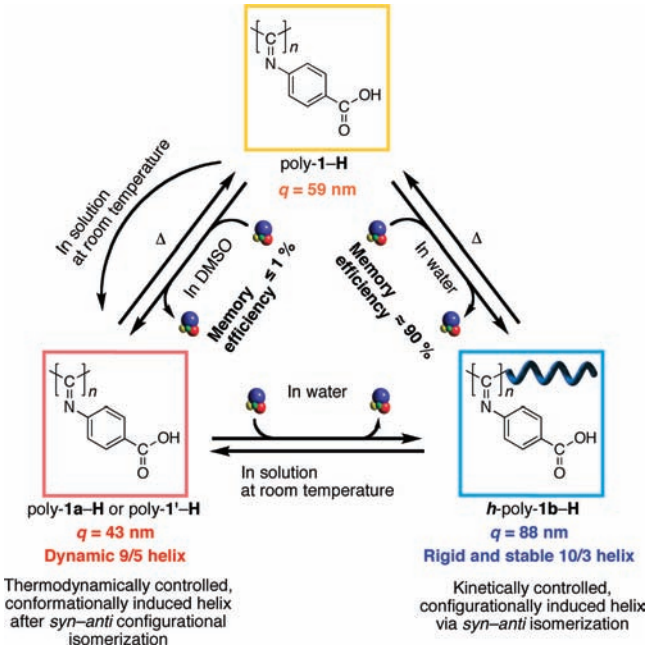

Figure 13. Possible structures of poly-**1**-**H**, poly-**1a**-**H**, poly-**1′**-**H**, and ***h***-poly-**1b**-**H** and their mutual interconversions.

rational isomerization of the C═N double bonds, going back to an analogous structure of poly-**1**-**H**.

The poly-**1**-**H** also folds into a preferred-handed rather semirigid 9/5 helical conformation composed of two monomer units as a repeating unit with an excess helical sense upon complexation with chiral amines in organic solutions and aqueous organic solutions containing less than 30 vol % water, as evidenced by the appearance of an ICD similar to that of ***h***-poly-**1b**-**H**,[19] arising from the similar *syn*−*anti* configurational isomerization. In sharp contrast to ***h***-poly-**1b**-**H**, however, the resulting helical conformation is dynamic in nature, different from that of ***h***-poly-**1b**-**H**, and may spontaneously racemize after removal of the chiral amines, as observed for the dynamically racemic polyacetylenes.[16a−i] Therefore, the induced helix in poly-**1a**-**H** is predominantly controlled by thermodynamics.[19] At high temperature, the poly-**1a**-**H** favorably changes to a structure similar to the original poly-**1**-**H** via configurational isomerization of the main-chain. The poly-**1a**-**H** structure may be among the thermodynamically most stable structures, since the "as-prepared" poly-**1**-**H** and kinetically produced ***h***-poly-**1b**-**H** also change their structures into a similar structure after being stored in solution for an extremely long time, and this was confirmed by following the changes in its ^{13}C NMR spectrum with time without heat treatment. In addition, upon complexation with chiral amines in water, a preferred-handed helix with a macromolecular helicity memory can also be induced in poly-**1a**-**H**.

Conclusions

In order to unravel the helicity induction mechanisms of the optically inactive poly(4-carboxyphenyl isocyanide) (poly-**1**-**H**) in DMSO and water with chiral amines and to address the question of why the helical structure induced in DMSO cannot be memorized after removal of the chiral amines (poly-**1a**-**H**), while that induced in water can be retained (***h***-poly-**1b**-**H**), a series of isotopically labeled poly-**1**-**H**'s and their methyl esters (poly-**1**-**Me**'s) with labeled with deuterium, ^{13}C, and ^{15}N and nonlabeled polymers were prepared, and their structures before and after the helicity induction with chiral amines in water and DMSO and subsequent memory were investigated in detail by absorption, CD, IR, VCD, and NMR spectroscopies together with XRD of the oriented films prepared from the nematic and cholesteric LC poly-**1**-**Me**'s, persistence length measurements, and theoretical calculations. From the spectroscopic measurement results, it has been concluded that the specific configurational isomerization around the C═N double bonds (*syn*−*anti* isomerism) occurs during the helicity induction processes in each solvent. XRD of the uniaxially oriented films of the corresponding methyl esters prepared from their LC polymer solutions suggests that the most plausible helical structure of poly-**1a**-**Me** is a 9/5 helix with two monomer units as a repeating unit, while that of ***h***-poly-**1b**-**Me** is a 10/3 helix consisting of one repeating monomer unit. The DFT calculations of poly(phenyl isocyanide), a model polymer of ***h***-poly-**1b**-**Me**, afford a 7/2 helix as the most possible helical structure, which is in good agreement with the XRD results. Furthermore, the persistence length (q) of poly-**1**-**Me** significantly increases from 59 to 88 nm once a preferred-handed helicity is induced and memorized (***h***-poly-**1b**-**Me**), whereas the q value of poly-**1a**-**Me**, which lost its optical activity after helicity induction, dramatically decreases to 43 nm, indicating a rather semirigid polymer. The variable-temperature NMR and CD spectra reveal that the polyisocyanides with different main-chain structures, poly-**1**-**H**, poly-**1a**-**H**, and ***h***-poly-**1b**-**H**, can interconvert in solution. The ***h***-poly-**1b**-**H** and poly-**1a**-**H**, with and without a helicity memory, respectively, favorably changed their helical structures to the original poly-**1**-**H** upon heating in solution via configurational isomerization of the main-chain. In addition, the original poly-**1**-**H** and ***h***-poly-**1b**-**H** also changed their structures into a structure analogous to that of poly-**1a**-**H** after standing in solution for an extremely long time without heat treatment. Upon complexation with chiral amines in water, a preferred-handed helix with a macromolecular helicity memory can also be induced in poly-**1a**-**H** in water. On the basis of these results together with the remarkable changes in the main-chain stiffness and the difference in the helical structures of poly-**1a**-**Me** and ***h***-poly-**1b**-**Me**, the mechanism of helix induction in poly-**1**-**H** with chiral amines in DMSO and water and the subsequent memory of the macromolecular helicity in water have been proposed as follows. In the presence of chiral amines in water, the original achiral poly-**1**-**H** folds into a rigid preferred-handed 10/3 helical structure, accompanied by transformation of an imino configurational mixture of *syn*- and *anti*-poly-**1**-**H** to one of a single configuration, and this selective configurational isomerization, driven by hydrophobic and chiral ionic interactions in water, assists the helical conformation on the polymer backbone to take an excess helical sense. Therefore, the induced helix is likely kinetically controlled and is retained after removal of the chiral amines at ambient temperature, while at high temperature the helical conformation unfolds due to the *syn*−*anti* configurational isomerization of the C═N double bonds, going back to the analogous structure of poly-**1**-**H**.

The poly-**1**-**H** also folds into a preferred-handed, semirigid 9/5 helical conformation with an excess helical sense upon complexation with chiral amines in DMSO, arising from the similar *syn*−*anti* configurational isomerization. In sharp contrast to ***h***-poly-**1b**-**H**, however, the resulting 9/5 helical conformation appears to be dynamic and spontaneously racemizes after removal of the chiral amines, as observed for dynamically racemic polyacetylenes. Therefore, the induced helix in poly-**1**-**H** is predominantly controlled by thermodynamics in DMSO.

The fact that the original poly-**1**-**H** and ***h***-poly-**1b**-**H** transform into the poly-**1a**-**H** at the end after standing in solution for an extremely long time supports the fact that the poly-**1a**-**H** structure may be the thermodynamically most stable structure. As a consequence, optically inactive poly(4-carboxyphenyl isocyanide) can adopt either a static or a dynamic helical conformation upon complexation with chiral amines in water or organic solvents, respectively, accompanied by selective configurational isomerization around the C═N double bonds, and these different helical conformations can interconvert. These findings combined with the previous discovery that the static helical polyisocyanides, once modified with achiral primary amines,[18] showed a significant improvement in thermal stability in water and organic solvents may be useful to design and construct novel functional chiral materials for chiral recognition and enantioselective catalysis[18b] due to the supramolecular helical array of the pendant functional groups.

Acknowledgment. This work was supported in part by a Grant-in-Aid for Scientific Research from the Japan Society for the Promotion of Science (JSPS), Japan Science and Technology Agency (JST), and the Global COE Program "Elucidation and Design of Materials and Molecular Functions" of the Ministry of Education, Culture, Sports, Science, and Technology, Japan. We thank Professors T. Yamane, A. Suzuki, and T. Hikage (Nagoya University) for their help in the X-ray diffraction measurements. We are deeply grateful to Dr. H. Kusanagi (ERATO, JST) for valuable discussions. We thank Mr. T. Miyabe for his assistance in the NMR measurements. K.N. expresses his thanks for a JSPS Research Fellowship for Young Scientists (No. 6683).

Supporting Information Available: Full experimental details; XRD data of HMW-poly-**1**-**Me**, HMW-***h***-poly-**1b**-**Me**, HMW-poly-**1a**-**Me**, and HMW-poly-**1′**-**Me**; ^{13}C NMR spectra of poly-**1**-**Me**-^{13}C, poly-**1′**-**Me**-^{13}C, ***h***-poly-**1b**-**Me**-^{13}C, and poly-**1a**-**Me**-^{13}C; IR spectra of poly-**1**-**Me**-^{13}C and poly-**1**-**Me**-^{15}**N**; VCD and IR spectra of ***h***-poly-**1b**-**Me**-d_4, ***h***-poly-**1b**-**Me**-^{13}C, ***h***-poly-**1b**-**Me**-d_4-^{13}C, and ***h***-poly-**1b**-**Me**-^{15}N and complete ref.[24] This material is available free of charge via Internet at http://pubs.acs.org.

JA904128D